

**Weighted Least Squares Topology Error Detection And  
Identification**

**A THESIS  
SUBMITTED TO THE FACULTY OF THE GRADUATE SCHOOL  
OF THE UNIVERSITY OF MINNESOTA  
BY**

**Jason Glen Lindquist**

**IN PARTIAL FULFILLMENT OF THE REQUIREMENTS  
FOR THE DEGREE OF  
Master of Science**

**Under the supervision of Bruce F. Wollenberg**

**November, 2010**

© Jason Glen Lindquist 2010  
ALL RIGHTS RESERVED

# Contents

<b>List of Tables</b>	<b>iv</b>
<b>List of Figures</b>	<b>v</b>
<b>1 Introduction</b>	<b>1</b>
<b>2 Weighted Least Squares State Estimation</b>	<b>3</b>
2.1 Transmission Network Model . . . . .	4
2.1.1 Transmission Lines . . . . .	4
2.1.2 Transformers . . . . .	4
2.1.3 Loads and Generators . . . . .	6
2.1.4 Topology Processor . . . . .	6
2.1.5 Bus Admittance Matrix, $Y$ . . . . .	6
2.2 Weighted Least Squares State Estimation . . . . .	7
2.2.1 Objective Function, $J$ . . . . .	7
2.2.2 Gain Matrix, $G$ . . . . .	8
2.2.3 State Vector, $x$ . . . . .	8
2.2.4 Normal Equation . . . . .	9
2.2.5 Measurement Function, $h(x)$ . . . . .	9
2.2.6 Measurement Jacobian, $H(x)$ . . . . .	10
2.2.7 Weighted Least Squares State Estimation Algorithm . . . . .	12
<b>3 Weighted Least Squares State Estimation Bad Data Processing</b>	<b>14</b>
3.1 Bad Data Detection and Identification . . . . .	15
3.2 Measurement Residuals . . . . .	17

3.3	Chi-Square Test . . . . .	21
3.4	Normalized Residuals Test . . . . .	23
3.5	Measurement Compensation And Normalized Residuals . . . . .	24
3.6	3-Bus Example . . . . .	26
3.7	Hypothesis Testing Identification Test . . . . .	29
<b>4</b>	<b>Topology Error Processing</b>	<b>38</b>
4.1	Topology Error Causes . . . . .	38
4.2	Topology Error Types . . . . .	39
4.3	Topology Error Effects . . . . .	42
4.4	Topology Error Detection . . . . .	44
4.5	Topology Error Processing Methods . . . . .	46
4.5.1	Generalized State Estimation . . . . .	47
4.5.2	Least Absolute Value State Estimation . . . . .	48
<b>5</b>	<b>Topology Error Detection and Identification Using WLS State Esti- mation</b>	<b>50</b>
5.1	Stage One: Topology Error Detection . . . . .	52
5.2	Stage Two: Topology Error Identification . . . . .	53
5.2.1	Topology Error Identification Criteria . . . . .	53
5.2.2	Topology Error Identification Processing . . . . .	54
<b>6</b>	<b>Topology Error Detection and Identification: MATLAB Simulation</b>	<b>58</b>
6.1	MATPOWER . . . . .	58
6.2	WLS State Estimator . . . . .	60
6.3	24-Bus IEEE Reliability Test System . . . . .	61
6.4	Topology Error Test Cases . . . . .	61
6.4.1	Branch Exclusion . . . . .	64
6.4.2	Branch Inclusion . . . . .	64
6.4.3	Bus Merge . . . . .	65
6.4.4	Bus Split . . . . .	66
6.4.5	Measurement Location and Topology Error . . . . .	66

6.4.6	Bad Measurement Data and Topology Error . . . . .	69
<b>7</b>	<b>Conclusion</b>	<b>81</b>
7.1	Further Research . . . . .	81
7.2	Advantages of the Method . . . . .	82
	<b>References</b>	<b>83</b>

# List of Tables

3.1	3-Bus Example System Parameters. . . . .	27
3.2	3-Bus Example. . . . .	28
3.3	Normalized Residual Test Example. . . . .	28
3.4	HTI Example Data. . . . .	30
4.1	Topology Error Example State Estimator Values. . . . .	43
6.1	Branch Exclusion Suspect Equipment. . . . .	64
6.2	Branch Inclusion Suspect Equipment. . . . .	65
6.3	Bus Merge Suspect Equipment. . . . .	67
6.4	Bus Split Suspect Equipment. . . . .	67
6.5	Bad Measurement Data On Branch 18. . . . .	69
6.6	Bad Data And Topology Error Suspect Equipment. . . . .	69
6.7	Branch Exclusion State Estimation Bad Data. . . . .	72
6.8	Branch Inclusion State Estimation Bad Data. . . . .	74
6.9	Bus Merge State Estimation Bad Data. . . . .	76
6.10	Bus Split State Estimation Bad Data. . . . .	76
6.11	Bad Data and Topology Error State Estimation Bad Data. . . . .	79

# List of Figures

2.1	Transmission Line Equivalent Circuit. . . . .	5
2.2	Transformer Equivalent Circuit. . . . .	5
2.3	Weighted Least Squares State Estimation Algorithm. . . . .	13
3.1	WLS State Estimation Algorithm With Bad Data Processing. . . . .	16
3.2	$\chi^2$ Plot With 100 Degrees of Freedom. . . . .	22
3.3	3-Bus Example. . . . .	26
3.4	HTI Example. . . . .	30
3.5	Hypothesis Test Identification Process. . . . .	31
3.6	Normal Distribution Plot, N(0,1). . . . .	32
3.7	Measurement Error Distribution, $N(e_{s_i}, \sigma_i^2(\Gamma_{ii} - 1))$ . . . . .	35
3.8	Error Distribution Plots, N(0,1). . . . .	35
3.9	Error Distribution and Decision Rules. . . . .	36
4.1	Breaker-And-A-Half Substation Configurations. . . . .	40
4.2	Breaker-And-A-Half Duplicate Substation Configurations. . . . .	41
4.3	Topology Error Example. . . . .	42
5.1	WLS Topology Error Identification And Detection. . . . .	51
5.2	Bus-Branch Model Inclusion Levels. . . . .	57
6.1	MATLAB Program Overview. . . . .	59
6.2	IEEE Reliability Test System. . . . .	62
6.3	IEEE Reliability Test System: Switch-Oriented Model. . . . .	63
6.4	Bus 9 Split Example. . . . .	68
6.5	Base Case MATPOWER PF and SE Solution. . . . .	70
6.6	Branch Exclusion MATPOWER PF and SE Solution. . . . .	71
6.7	Branch Inclusion MATPOWER PF and SE Solution. . . . .	73

6.8	Bus Merge MATPOWER PF and SE Solution. . . . .	75
6.9	Bus Split MATPOWER PF and SE Solution. . . . .	77
6.10	Bad Data And Topology Error MATPOWER PF and SE Solution. . . . .	78
6.11	Undetectable Bus Split Topology Error. . . . .	80



# Chapter 1

## Introduction

Within a power system control center is an Energy Management System that monitors the power system. The primary tool used to monitor the transmission network is the state estimator. The state estimator uses a model of the transmission network and a set of measurements to obtain an estimate of the operating state. It is possible for the model used by the state estimator to not match the physical system, containing a topology error, and result in an incorrect estimate of the operating state. Topology error detection and identification is the process of correcting this type of state estimation error. The goal of this work is to detect and identify inconsistencies between the model used by the state estimator and the physical system using Weighted Least Squares State Estimation.

The power system state estimator uses a bus-branch model of the transmission network, a system of equations and a set of measurements to obtain an estimate of the operating state. The bus-branch model is a high-level model that reduces the physical system to buses and branches. The system of equation defines the relationship between the bus-branch model and bus voltages, bus injections and branch flows. The measurement set includes branch flow, bus injection and bus voltage magnitudes. The state estimator combines these to obtain an accurate estimate of the operating state of the transmission network. Any time one of these components are incorrect, the state estimate no longer gives an accurate estimate of the system operating point.

The effect of a topology error on the state estimation solution is an increase in measurement residuals near the topology error and an increase in the objective function

value. This effect can be exploited to both detect and identify incorrect topology in the model. The existence of a topology error is detected by the state estimation bad data processing. The cause of the topology error is identified by adjusting the topology model and performing additional state estimate runs to determine the model that results in the minimum objective function value.

After the state estimator converges, the measurements identified as bad can be analyzed to determine if a topology error is suspect to exist in the bus-branch model. If a topology error is suspect, additional processing can be done to identify the topology error or to verify that a topology error does not exist. This subsequent processing begins by identifying the portion of the network where the topology error is suspect. The bus-branch model is reduced around the suspect topology error and further analyzed. This analysis includes identifying each valid bus-branch configuration in the reduced model and obtaining a state estimation solution for each of these configuration. The correct bus-branch model can then be identified by comparing the objective values for each solution. The correct bus-branch model will correspond to the solution with the minimum objective value. As result, the topology error will now be identified and the bus-branch model used by the state estimator can be corrected, allowing an accurate estimate of the system operating point can be obtained.

The details of this process along with a MATLAB implementation and examples are now presented.

- Chapter 2 presents conventional power system state estimation.
- Chapter 3 power system state estimation bad data processing.
- Chapter 4 gives an overview of topology error processing.
- Chapter 5 describes the proposed method of topology error processing.
- Chapter 6 presents the MATLAB implementation and examples of the proposed method of topology error processing.
- Chapter 7 contains the conclusions of this research.

## Chapter 2

# Weighted Least Squares State Estimation

Power system state estimation (SE) has a primary role in an Energy Management System (EMS) as a real-time monitoring tool [1]. The purpose of power system SE is to provide a reliable state estimate of the operating state of an electric power system from a redundant set of measurements [2, 3]. The static state of a transmission network includes a complete set of bus voltage magnitudes and angles. From this, all other system quantities can be calculated, including power flows, power injections and current flows.

A SE solution is based on a network model and a redundant set of measurements. The static network model includes the network and substation topology model and parameters. The dynamic measurement data include the analog and digital measurements. The analog measurements consist of bus voltage magnitudes and the real and reactive power flows and power injections. The measurements are collected from the measuring devices by Remote Terminal Units (RTUs) and a SCADA (Supervisory Control And Data Acquisition) system. The digital measurements consist of switch statuses and tap positions. A system of equations and parameters defines the relationship between the bus-branch network model and bus voltages, bus injections and branch flows.

An accurate estimate of the system state can be obtained from a set of sufficiently redundant measurements and a valid model of the system. The SE program processes the measurement and network data to provide an optimal estimate of the current state of

the system. The primary tool used to obtain a power system state estimate is Weighted Least Squares (WLS) SE. WLS SE seeks to determine the optimal state estimate for a given set of measurements by minimizing the weighted sum of calculated error. The error is the difference between the measured values and the estimated system values derived from the estimate of the system states.

## 2.1 Transmission Network Model

The first step in WLS SE is to build a bus-branch network model of the system. The model is based on the assumption that the power system operates in the steady state under balanced conditions (i.e. all loads and branch power flows are three phase and balanced). From this assumption, the model can be built using a single phase positive sequence equivalent circuit where all the network data and variables are defined according to the per unit system [4]. The network topology processor builds the network model by combining digital and analog measurements, network parameters and equipment connectivity.

### 2.1.1 Transmission Lines

Transmission lines are modeled by a two-port  $\pi$ -model with a series impedance  $z = r + jx$  and total line charging susceptance  $j2B$  [5]. The branch admittance is derived from the series impedance.

$$y = z^{-1} = g + jb$$

The series conductance,  $g$ , and the series susceptance,  $b$ , are defined as

$$\begin{aligned} g &= \frac{r}{r^2 + x^2} \\ b &= -\frac{x}{r^2 + x^2} \end{aligned}$$

### 2.1.2 Transformers

Transformers are modeled as an ideal transformer with a phase tap ratio  $a$  and a series impedance of  $r + jx$  (figure 2.2).

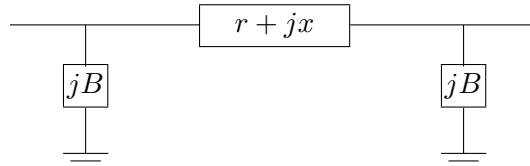


Figure 2.1: Transmission Line Equivalent Circuit.

To derive the nodal equations begin with the current flows  $i_{lm}$  and  $i_m$  and denote the  $l$ - $m$  branch admittance by  $y$ .

$$\begin{bmatrix} i_{lm} \\ i_m \end{bmatrix} = \begin{bmatrix} y & -y \\ -y & y \end{bmatrix} \begin{bmatrix} v_l \\ v_m \end{bmatrix}$$

Next, substitute  $i_{lm}$  and  $v_l$  to obtain the final form of equation (2.1):

$$\begin{aligned} i_{lm} &= a i_k \\ v_l &= a v_k \end{aligned}$$

$$\begin{bmatrix} i_k \\ i_m \end{bmatrix} = \begin{bmatrix} y/a^2 & -y/a \\ -y/a & y \end{bmatrix} \begin{bmatrix} v_k \\ v_m \end{bmatrix} \quad (2.1)$$

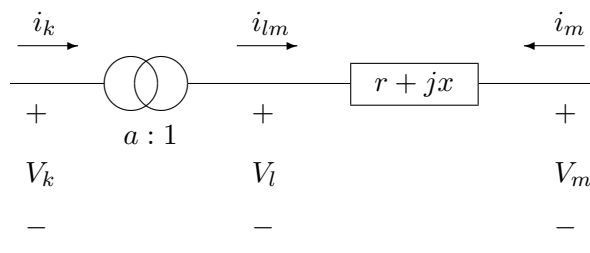


Figure 2.2: Transformer Equivalent Circuit.

### 2.1.3 Loads and Generators

Loads and generators are modeled as complex power injections at the station bus with power flowing into a bus being positive and power flowing out of a bus being negative. A generator has a positive injection value and a load has a negative injection value.

### 2.1.4 Topology Processor

The topology processor determines the connectivity of the network and define the location of measurements [3]. The topology processor determines the connectedness of the model from system telemetry which is retrieved via a SCADA system. This telemetry includes both analog and digital measurements. The topology processor reduces the physical model to a bus-branch model to be used by the SE program.

### 2.1.5 Bus Admittance Matrix, $Y$

The connectivity of the network model components is defined by the bus admittance matrix,  $Y$ . This admittance matrix is a complex, symmetric matrix that defines the relationship between net current injections and bus voltage phasors. The diagonal elements are the sum of admittances connected to bus  $k$  and called *self-admittance*. The off-diagonal elements are the negative of the sum of admittances connected between bus  $k$  and  $m$  and called *mutual admittance*.

$$\begin{aligned} I &= Y \cdot V \\ Y &= G + jB \end{aligned}$$

The bus admittance matrix is built by adding components one at a time [5]. To add a component connected between bus  $k$  and  $m$  with admittance  $y$  and tap ratio  $a$ , update the four respective entries of  $Y$ :

$$\begin{aligned} Y_{kk}^{new} &= Y_{kk}^{old} + y/a^2 \\ Y_{km}^{new} &= Y_{km}^{old} + y/a \\ Y_{mk}^{new} &= Y_{mk}^{old} + y/a \\ Y_{mm}^{new} &= Y_{mm}^{old} + y \end{aligned}$$

This matrix is used to calculate the bus real and reactive power injections.

## 2.2 Weighted Least Squares State Estimation

The goal of SE is to determine the most probable state of an electric power system given a redundant set of measurements [5]. In WLS SE, the most probable state is defined as the state that minimizes the WLS objective function. The minimum of the objective function is obtained by using the Gauss-Newton method, which iteratively updates the estimate through a linearization of the system.

### 2.2.1 Objective Function, $J$

A SE solution is obtained by minimizing the WLS objective function:

$$J(x) = [z - h(x)]^T R_z^{-1} [z - h(x)] \quad (2.2)$$

$z$ : vector of measurements

$h(x)$ : measurement function

$x$ : state vector

$R_z$ : measurement error covariance matrix.

$[z - h(x)]$ : residual vector

The measurement error covariance matrix,  $R_z$ , is a diagonal matrix of measurement variances used as the weights. It is possible to use a WLS approach to obtain an optimal estimate because it is assumed that the measurement errors,  $e$ , are Gaussian and independent.

$$E(e_i) = 0$$

$$E(e \cdot e^T) = R_z$$

$$R_z = \begin{bmatrix} \sigma_1^2 & 0 & \dots & 0 & 0 \\ 0 & \sigma_2^2 & & 0 & 0 \\ \vdots & \vdots & \ddots & \vdots & \vdots \\ 0 & 0 & \dots & \sigma_{m-1}^2 & 0 \\ 0 & 0 & \dots & 0 & \sigma_m^2 \end{bmatrix}$$

An optimal estimate is obtained by minimizing the objective function by taking the

gradient vector of the objective function and setting it equal to zero [6].

$$\left. \frac{\partial J(x)}{\partial x} \right|_{x=\hat{x}} = 0$$

$$\frac{\partial J(x)}{\partial x} = -2H^T R_z^{-1} [z - h(x)] = 0$$

The Measurement Jacobian matrix,  $H$ , is defined as

$$H(x) = [\partial h(x)/\partial x] \quad (2.3)$$

The Gauss-Newton method is used to iteratively obtain a SE solution. This is based on taking the first order terms of the Taylor expansion of (2.3):

$$g(x^{k+1}) = g(x^k) + G(x^k)(x^{k+1} - x^k) + \dots = 0$$

The iterative solution of  $x$  is obtained by ignoring the higher order terms and solving for  $x^{k+1}$  at each iteration  $k$  where  $G(x)$  is the Gain Matrix and  $x$  is the state vector.

$$x^{k+1} = x^k - G(x^k)^{-1}g(x^k)$$

### 2.2.2 Gain Matrix, $G$

When the system is fully observable the gain matrix is a symmetric positive definite sparse matrix [5].<sup>1</sup>

$$G = H^T R_z^{-1} H \quad (2.4)$$

From one iteration to the next, the change in the gain matrix,  $G$ , is negligible to the point that the gain matrix can be calculated one time for all iterations [8].

### 2.2.3 State Vector, $x$

The state vector consists of  $(2N - 1)$  elements, including  $(N - 1)$  phase angles and  $N$  bus voltage magnitudes, where  $N$  is the number of network buses. The phase angle of the reference bus is set to 0 and excluded from the state vector.

<sup>1</sup> A system state is observable when it can be estimated from the given measurement set [7].



$$x = [\theta_2, \theta_3, \dots, \theta_n, V_1, V_2, \dots, V_n]^T$$

- x: state vector
- $V_i$ : bus  $i$  voltage magnitude
- $\theta_i$ : bus  $i$  phase angle
- n: number of network buses

### 2.2.4 Normal Equation

The Normal Equation, equation (2.5), are used to solve for the change in the state vector,  $\Delta x$ .

$$G(x^k) \Delta x^{k+1} = H(x^k)^T R_z^{-1} [z - h(x^k)] \quad (2.5)$$

- k: iteration index
- $\Delta x^{k+1} = x^{k+1} - x^k$

### 2.2.5 Measurement Function, $h(x)$

The measurement set includes branch power flows, bus injections and bus voltage magnitudes. The relationship between complex bus voltages and the measurements are defined by the measurement function's set of equations. Each measurement corresponds to a single entry in the measurement function vector,  $h(x)$ . The dimensions of the measurement function is  $m \times n$  where  $m$  is the number of measurements and  $n$  is the number of states.

Real and reactive power injection measurements:

$$P_i = V_i \sum_{j \in N_i} V_j (G_{ij} \cos \theta_{ij} + B_{ij} \sin \theta_{ij})$$

$$Q_i = V_i \sum_{j \in N_i} V_j (G_{ij} \sin \theta_{ij} - B_{ij} \cos \theta_{ij})$$

Real and reactive power flow measurements:

$$P_{ij} = V_i^2 g_{ij} - V_i V_j (g_{ij} \cos \theta_{ij} + b_{ij} \sin \theta_{ij})$$

$$Q_{ij} = -V_i^2 (b_{si} + b_{ij}) - V_i V_j (g_{ij} \sin \theta_{ij} - b_{ij} \cos \theta_{ij})$$

- $V_i$ : bus  $i$  voltage magnitudes  
 $\theta_i$ : bus  $i$  phase angle  
 $\theta_{ij} = \theta_i - \theta_j$   
 $g_{ij} + jb_{ij}$ : branch connecting buses  $i$  and  $j$  admittance  
 $G_{ij} + jB_{ij}$ : mutual admittance between buses  $i$  and  $j$  where  $i \neq j$   
 $G_{ii} + jB_{ii}$ : self admittance at bus  $i$   
 $b_{si}$ : susceptance of bus  $i$   
 $N_i$ : set of buses directly connected to bus  $i$

The power flow equations are derived from Kirchoff's current law and the nodal equations. <sup>2</sup>

### 2.2.6 Measurement Jacobian, $H(x)$

The measurement Jacobian matrix, equation (2.6), is the partial derivative of the measurement function,  $h(x)$ , with respect to the state vector,  $x$ .

$$H(x) = [\partial h(x)/\partial x] \quad (2.6)$$

---

2

$$\begin{aligned}
S_i = P_i + jQ_i &= \vec{V}_i \vec{I}_i^* = \vec{V}_i \left[ \sum_{j \in N_j} Y_{ij} \vec{V}_j \right]^* = V_i \sum_{j \in N_j} (G_{ij} - jB_{ij}) V_j e^{j(\theta_i - \theta_j)} \\
&= V_i \sum_{j \in N_j} V_j [G_{ij} \cos \theta_{ij} + B_{ij} \sin \theta_{ij}] + jV_i \sum_{j \in N_j} V_j [G_{ij} \sin \theta_{ij} - B_{ij} \cos \theta_{ij}] \\
S_{ij} = P_{ij} + jQ_{ij} &= \vec{V}_i \vec{I}_{ij}^* = \vec{V}_i \left[ y_{ij} (\vec{V}_i - \vec{V}_j) + y_{si} \vec{V}_i \right]^* \\
&= V_i e^{j\theta_i} \left[ y_{ij} (V_i e^{j\theta_i} - V_j e^{j\theta_j}) + y_{si} V_i e^{j\theta_i} \right]^* \\
&= V_i \left[ (g_{ij} - jb_{ij}) (V_i - V_j e^{j\theta_{ij}}) + (g_{si} - jb_{si}) V_i \right] \\
&= [V_i^2 (g_{ij} + g_{si}) - V_i V_j (g_{ij} \cos \theta_{ij} + b_{ij} \sin \theta_{ij})] \\
&\quad + j [-V_i^2 (b_{ij} + b_{si}) - V_i V_j (g_{ij} \sin \theta_{ij} - b_{ij} \cos \theta_{ij})]
\end{aligned}$$

$$H = \begin{bmatrix} \frac{P_{inj}}{\partial\theta} & \frac{P_{inj}}{\partial V} \\ \frac{P_{flow}}{\partial\theta} & \frac{P_{flow}}{\partial V} \\ \frac{Q_{inj}}{\partial\theta} & \frac{Q_{inj}}{\partial V} \\ \frac{Q_{flow}}{\partial\theta} & \frac{Q_{flow}}{\partial V} \\ 0 & \frac{V_{mag}}{\partial V} \end{bmatrix}$$

The elements of the measurement Jacobian matrix are defined as follows:

$$\frac{\partial P_i}{\partial\theta_i} = \sum_{j \in N_i} V_i V_j (-G_{ij} \sin\theta_{ij} + B_{ij} \cos\theta_{ij}) - V_i^2 B_{ii}$$

$$\frac{\partial P_i}{\partial\theta_j} = V_i V_j (G_{ij} \sin\theta_{ij} - B_{ij} \cos\theta_{ij})$$

$$\frac{\partial P_i}{\partial V_i} = \sum_{j \in N_i} V_j (G_{ij} \cos\theta_{ij} + B_{ij} \sin\theta_{ij}) + V_i G_{ii}$$

$$\frac{\partial P_i}{\partial V_j} = V_i (G_{ij} \cos\theta_{ij} + B_{ij} \sin\theta_{ij})$$

$$\frac{\partial Q_i}{\partial\theta_i} = \sum_{j \in N_i} V_i V_j (G_{ij} \cos\theta_{ij} + B_{ij} \sin\theta_{ij}) - V_i^2 G_{ii}$$

$$\frac{\partial Q_i}{\partial\theta_j} = V_i V_j (-G_{ij} \cos\theta_{ij} - B_{ij} \sin\theta_{ij})$$

$$\frac{\partial Q_i}{\partial V_i} = \sum_{j \in N_i} V_j (G_{ij} \sin\theta_{ij} + B_{ij} \cos\theta_{ij}) + V_i B_{ii}$$

$$\frac{\partial Q_i}{\partial V_j} = V_i (G_{ij} \sin\theta_{ij} + B_{ij} \cos\theta_{ij})$$

$$\begin{aligned}
\frac{\partial P_{ij}}{\partial \theta_i} &= V_i V_j (g_{ij} \sin \theta_{ij} - b_{ij} \cos \theta_{ij}) \\
\frac{\partial P_{ij}}{\partial \theta_j} &= -V_i V_j (g_{ij} \sin \theta_{ij} - b_{ij} \cos \theta_{ij}) \\
\frac{\partial P_{ij}}{\partial V_i} &= -V_j (g_{ij} \cos \theta_{ij} + b_{ij} \sin \theta_{ij}) + 2V_i (g_{ij} + g_{si}) \\
\frac{\partial P_{ij}}{\partial V_j} &= -V_i (g_{ij} \cos \theta_{ij} + b_{ij} \sin \theta_{ij}) \\
\\
\frac{\partial Q_{ij}}{\partial \theta_i} &= -V_i V_j (g_{ij} \cos \theta_{ij} - b_{ij} \sin \theta_{ij}) \\
\frac{\partial Q_{ij}}{\partial \theta_j} &= V_i V_j (g_{ij} \cos \theta_{ij} - b_{ij} \sin \theta_{ij}) \\
\frac{\partial Q_{ij}}{\partial V_i} &= -V_j (g_{ij} \sin \theta_{ij} - b_{ij} \cos \theta_{ij}) - 2V_i (b_{ij} + b_{si}) \\
\frac{\partial Q_{ij}}{\partial V_j} &= -V_i (g_{ij} \sin \theta_{ij} - b_{ij} \cos \theta_{ij})
\end{aligned}$$

$$\begin{aligned}
\frac{\partial V_i}{\partial V_i} &= 1 \\
\frac{\partial V_i}{\partial V_j} &= 0 \\
\frac{\partial V_i}{\partial \theta_i} &= 0 \\
\frac{\partial V_i}{\partial \theta_j} &= 0
\end{aligned}$$

### 2.2.7 Weighted Least Squares State Estimation Algorithm

An iterative algorithm is used to obtain a WLS SE solution based on the Gauss-Newton method, figure 2.3. At step 1 the iteration counter is set to 0 and the state vector is initialized to 0.0 degrees for bus angles and to 1.0 p.u. for bus voltage magnitudes. In step 2 the Jacobian matrix is calculated,  $H$ . In subsequent iterations this step can be bypassed to increase convergence time.<sup>3</sup> Step 3 is the first part in solving the normal equations and step 4 obtains the iterative solution. Step 5 tests for convergence, which

<sup>2</sup> The Jacobian matrix does not change significantly from each iteration. In steady state operation the angle difference between buses,  $\theta_{ij}$ , tends to be near 0.0 radians and the bus voltage magnitudes are near 1.0 p.u..

is obtained when the largest change in the state variable is smaller than a user-defined threshold. If the SE algorithm converged, the process stops. Otherwise, the state vector is updated in step 6 and the iterative process continues. At the completion of the algorithm, an accurate state estimate is obtained and the operating point of the system can be determined.

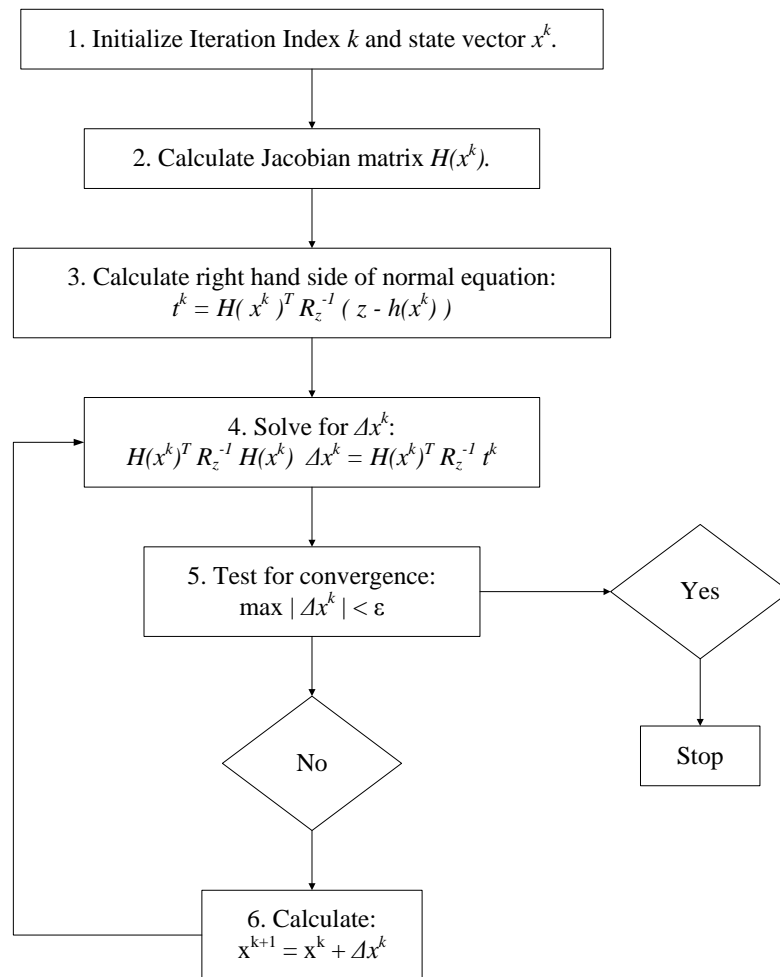


Figure 2.3: Weighted Least Squares State Estimation Algorithm.

## Chapter 3

# Weighted Least Squares State Estimation Bad Data Processing

An essential component of power system SE is the detection, identification and removal of bad data. The causes of gross measurement errors can include incorrect meter polarity<sup>1</sup> and settings, imbalance in three-phase power flow, incorrect transformer tap settings, incorrect branch impedance parameter values and communication network errors [9]. The sources of bad data can be grouped into three categories: measurements, topology and parameters. In conventional power system SE only measurement errors are handled and the system topology and network parameters are assumed to be accurate. This assumption is often valid and allows for a well defined SE algorithm.

Bad data in the measurement set refers to bad measurements that do not fit with the rest of the measurement set [6]. Stated slightly differently, bad data is a measurement with an error larger than the known accuracy of the meter [10]. This is different than measurement noise, which can be filtered by the WLS SE algorithm. When the results of SE do not match the accuracy of the measurement standard deviations, a conclusion is made that the measurements contain gross errors [3]. Given sufficient measurement redundancy, measurement errors can be detected, identified and removed from the measurement set.

---

<sup>1</sup> One convention used in transmission network SE is for the flow into a node to be positive. This is not always the case at the source or provider of the analog telemetry measurements [9].

### 3.1 Bad Data Detection and Identification

Detection of bad data is the process of determining if bad data exist in the measurement set. Identification of bad data is the process of determining which measurements contain bad data [5]. Once bad data is identified it can be removed from the measurement set and a new SE solution can be obtained that is free of bad data.

Bad data processing is dependent on a system's measurement redundancy and measurement placement. The definitions of critical measurements are

- Critical Measurement: if removed makes the system unobservable
- Critical Pair of Measurements: if one of the measurements is removed the other measurement becomes critical
- Critical Set of Measurements: if the set is removed, the system becomes unobservable

Bad data that corresponds to a critical measurement is not detectable and bad data in a critical set is not identifiable [11].

The effect of gross measurement errors on WLS SE is dependant on measurement redundancy. In highly redundant areas the effect tends to be localized to the bad data. In low redundant areas the residuals of neighboring measurements are affected [9]. This is commonly referred to as the "smearing" effect. One method to minimize this is to add zero-injection measurements. These are zero MW and MVAR pseudo-measurements at buses with no load or generation. The result of this is to localize the influence of a bad measurement to an adjacent bus in the area of low redundancy [9].

The bad data processor should be able to handle multiple types of bad data. Beyond single bad data, multiple bad data can occur as either interacting or non-interacting and conforming or non-conforming. The algorithm presented in figure 2.3 does not include bad data processing. In a WLS SE program, bad data processing occurs after convergence, figure 3.1.

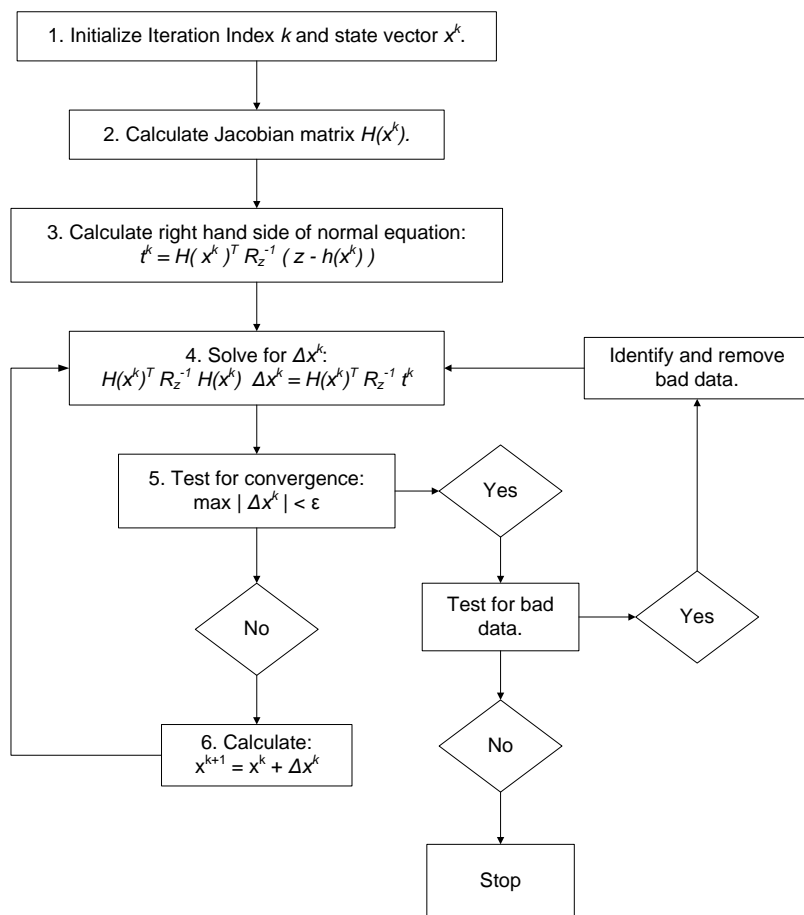


Figure 3.1: WLS State Estimation Algorithm With Bad Data Processing.



## 3.2 Measurement Residuals

In WLS SE, bad data processing occurs after convergence by processing the measurement residuals and the associated covariance matrix. This involves deriving the residual equations and performing a sensitivity analysis to obtain the covariance matrix.

To derive the measurement residual equations, start with the linearized measurement equation.

$$\begin{aligned}\Delta z &= H\Delta x + e \\ E[e] &= 0 \\ COV[e] &= R_z\end{aligned}\tag{3.1}$$

The WLS estimator solution to the linearized measurement equation (3.1) gives

$$\begin{aligned}\Delta \hat{x} &= (H^T R_z^{-1} H)^{-1} H^T R_z^{-1} \Delta z \\ &= G^{-1} H^T R_z^{-1} \Delta z\end{aligned}\tag{3.2}$$

Equation (3.2) gives the sensitivity matrix of the state estimate in respect to the measurements.

$$\frac{\partial \hat{x}}{\partial z} = G^{-1} H^T R_z^{-1}$$

To find the relationship between  $\Delta \hat{z}$  and  $\Delta z$  begin with the measurement equation and Jacobian (2.3).

$$\begin{aligned}z &= h(x) + e \\ \frac{\partial z}{\partial x} &= \frac{\partial h(x)}{\partial x} + 0 = H(x)\end{aligned}\tag{3.3}$$

Use equation (3.3) and (3.2) to relate  $\Delta \hat{z}$  and  $\Delta z$ .

$$\begin{aligned}\Delta \hat{z} &= H\Delta \hat{x} \\ &= H \cdot G^{-1} H^T R_z^{-1} \Delta z \\ &= K\Delta z\end{aligned}\tag{3.4}$$

Matrix  $K$  is defined as the measurement sensitivity matrix.

$$\begin{aligned}K &= \frac{\partial \hat{z}}{\partial z} \\ &= H G^{-1} H^T R_z^{-1} \\ &= H \frac{\partial \hat{x}}{\partial z}\end{aligned}\tag{3.5}$$

The  $K$  matrix has the following properties. <sup>2</sup>

$$K \cdot K \cdot K \cdots K = K \quad (3.6)$$

$$K \cdot H = H \quad (3.7)$$

$$(I - K)H = 0 \quad (3.8)$$

The sensitivity of the residual estimate to measurements is derived from the residual estimate based on the linearized measurement equation. This simplification is justified because the effect of noise on the measurement residual tends to be nearly linear [12]. <sup>3</sup>

$$\hat{r} = z - H\hat{x} \quad (3.9)$$

$$\Delta\hat{r} = \Delta z - H\Delta\hat{x} \quad (3.10)$$

---

<sup>2</sup> The first and second properties can be derived by expanding  $K$  using (3.5) and then expanding  $G$  using (2.4).

$$\begin{aligned} K \cdot K \cdot K \cdots K &= HG^{-1}H^T R_z^{-1} \cdot HG^{-1}H^T R_z^{-1} \cdot K \cdots K \\ &= H \left( H^T R_z^{-1} H \right)^{-1} H^T R_z^{-1} \cdot HG^{-1}H^T R_z^{-1} \cdot K \cdots K \\ &= HG^{-1}H^T R_z^{-1} \cdot K \cdots K \\ &\vdots \\ &= H \left( H^T R_z^{-1} H \right)^{-1} H^T R_z^{-1} \cdot HG^{-1}H^T R_z^{-1} \\ &= HG^{-1}H^T R_z^{-1} \\ &= K \end{aligned}$$

$$\begin{aligned} K \cdot H &= HG^{-1}H^T R_z^{-1} \cdot H \\ &= H \left( H^T R_z^{-1} H \right)^{-1} H^T R_z^{-1} \cdot H \\ &= H \end{aligned}$$

<sup>3</sup>

$$r = z - h(\hat{x})$$

Apply perturbation  $\Delta\hat{x}$  to  $\hat{x}$ .

$$\begin{aligned} r^{new} &= r + \Delta r \\ &= z + \Delta z - h(\hat{x} + \Delta\hat{x}) \end{aligned}$$

From equations (3.10) and (3.2) the residual sensitivity matrix  $S = \partial\hat{r}/\partial z$  can be derived.

$$\begin{aligned}\Delta\hat{r} &= \Delta z - H\Delta\hat{x} \\ &= \Delta z - HG^{-1}H^T R_z^{-1}\Delta z \\ &= (I - HG^{-1}H^T R_z^{-1})\Delta z \\ \frac{\partial\hat{r}}{\partial z} &= I - HG^{-1}H^T R_z^{-1} \\ &= I - \frac{\partial\hat{z}}{\partial z}\end{aligned}$$

The residual sensitivity matrix,  $S = \frac{\partial\hat{r}}{\partial z} = I - K$ , is defined by the measurement residual equation and gives a measure of the sensitivity of residuals to measurement errors [5]. This is an approximation because it is based on the linear measurement equation. <sup>4</sup>

$$\hat{r} = Se \tag{3.11}$$

Equation (3.11) shows that residual estimate is a weighted sum of measurement errors where the sensitivity matrix,  $S$ , provides the weights. The sensitivity matrix has a rank of  $k = m - n$ . If a critical measurement exists, the column in  $S$  will be zero, corresponding to the critical measurement. A column corresponding to critical sets of measurements will be linearly dependent in  $S$  [11].

---

Use the linear approximation

$$h(\hat{x} + \Delta\hat{x}) \approx h(\hat{x}) + H\Delta\hat{x}$$

giving

$$\begin{aligned}r + \Delta r &= z + \Delta z - h(\hat{x}) - H\Delta\hat{x} \\ &= r + \Delta z - H\Delta\hat{x}\end{aligned}$$

therefore

$$\Delta r = \Delta z - H\Delta\hat{x}$$

4

$$r = z - \hat{z}$$

Apply linear approximation

$$\begin{aligned}z &= Hx + e \\ \hat{z} &= H\hat{x}\end{aligned}$$

The distribution of the measurement residuals can be derived from the definition of expected value and covariance and equation (3.11).<sup>5</sup>

$$\begin{aligned} E[r] &= 0 \\ COV[r] &= S \cdot R_z \cdot S^T \end{aligned} \tag{3.12}$$

$$= S \cdot R_z \tag{3.13}$$

Equation (3.12) is reduced to (3.13) by using equation (3.8) and the definition of  $R_z$  as a symmetric matrix.<sup>6</sup> Therefore the measurement residual,  $r$ , has a normal distribution with a mean of zero and a variance of  $R_{\hat{r}} = S \cdot R_z$ .

$$r \sim N(0, R_{\hat{r}})$$

and the WLS solution to (3.11),  $x = G^{-1}H^T R_z^{-1}z$

$$\begin{aligned} r &= z - H\hat{x} \\ &= z - HG^{-1}H^T R_z^{-1}z \\ &= (I - HG^{-1}H^T R_z^{-1})z \\ &= (I - HG^{-1}H^T R_z^{-1})(Hx + e) \\ &= (H - HG^{-1}H^T R_z^{-1}H)x + Se \\ &= (H - HG^{-1}G)x + Se \\ &= (0)x + Se \\ &= Se \end{aligned}$$

5

$$\begin{aligned} E[r] &= E(S \cdot e) = S \cdot E(e) = 0 \\ COV[r] &= E[r \cdot r^T] \\ &= E[Se \cdot (Se)^T] \\ &= E[Se \cdot e^T S^T] \\ &= S \cdot E[e \cdot e^T] \cdot S^T \\ &= S \cdot R_z \cdot S^T \end{aligned}$$

### 3.3 Chi-Square Test

A statistical method of bad data detection is the chi-square,  $\chi^2$ , test. A  $\chi^2$  distribution with  $k$  degrees of freedom is the distribution of the sum of squares of  $k$  independent and normally distributed random variables. It can be used to test if a distribution is normal and provides a quantitative means to test a hypothesis [13]. In the case of WLS SE the  $\chi^2$  test determines if the objective function, equation (2.2), fits a normal distribution. When no bad data exist in the measurement set and the measurement errors follow a normal distribution, the objective  $J(x)$  follows a  $\chi^2$  distribution with  $m - n$  degrees of freedom [6].

A  $\chi^2$  distribution with  $k$  degrees of freedom,  $Y \sim \chi_k^2$ , has the following form:

$$Y = \sum_{i=1}^k X_i^2$$

Each  $X_i$  is an independent random variable and the summation can be applied to the SE objective function, which is an approximation of a  $\chi^2$  distribution (2.2).

$$J(x) = \sum_{i=1}^m \frac{e_i^2}{R_z(ii)} \quad (3.14)$$

The quantity  $\frac{e_i^2}{R_z(ii)}$  has a standard normal distribution and can be applied to the  $\chi^2$  test. The  $k$  degrees of freedom is equal to the number of measurements minus the number of states,  $m - n$  [5]. The objective function follows a  $\chi^2$  distribution with  $m - n$  degrees

---

6

$$\begin{aligned}
COV[r] &= S \cdot R_z \cdot S^T \\
&= (I - K) \cdot R_z \cdot (I - K)^T \\
&= (I - K) \cdot R_z \cdot (I - K^T) \\
&= (I - K) R_z - (I - K) R_z K^T \\
&= (I - K) R_z - (I - K) R_z (HG^{-1}H^T R_z^{-1})^T \\
&= (I - K) R_z - (I - K) R_z (R_z^{-1})^T (HG^{-1}H^T)^T \\
&= (I - K) R_z - (I - K) R_z R_z^{-1} H (G^{-1})^T H^T \\
&= (I - K) R_z - (I - K) H (G^{-1})^T H^T \\
&= (I - K) R_z - 0 \\
COV[r] &= S \cdot R_z
\end{aligned}$$

of freedom when the measurement set is free of bad data and the measurement errors have a normal distribution [6].

Bad data is suspected if the objective function exceeds the  $\chi^2$  distribution for a given confidence level. A confidence level (e.g. 95%) is chosen for a given system and the threshold value is determined from a  $\chi^2$  probability density function with  $m - n$  degrees of freedom. If the objective function value exceeds this threshold, then bad data will be suspected. Otherwise, it is assumed that the measurement set is free of bad data.

Figure 3.2 shows the plots of the probability density function, PDF, and the cumulative distribution function, CDF, for a  $\chi^2$  distribution with 100 degrees of freedom. On both of the plots the 95% confidence interval is marked. For a WLS SE with a deference between the number of states and the number of measurements equal to 100, bad data will not be suspected until the normalized objective function value exceeds 124.3.

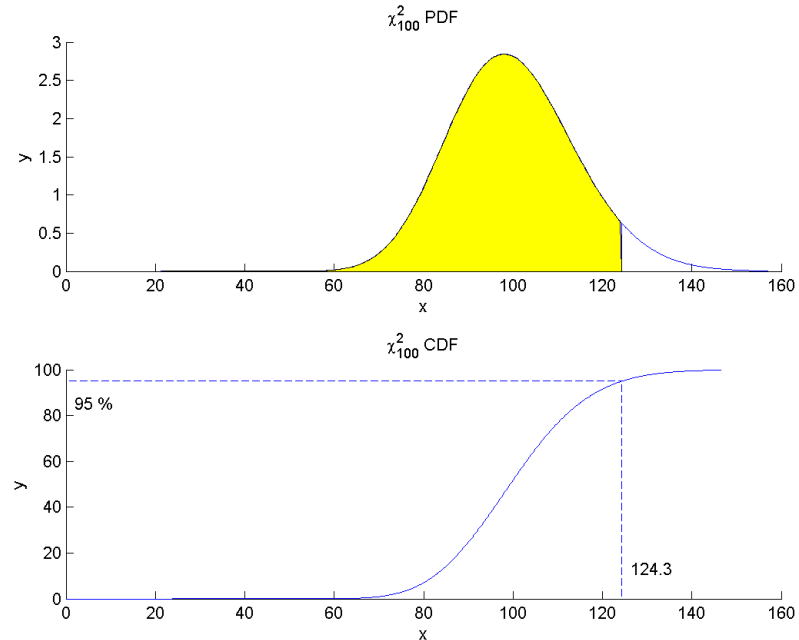


Figure 3.2:  $\chi^2$  Plot With 100 Degrees of Freedom.

It is possible for bad data to go undetected by the  $\chi^2$  test. The reason for this is that the degrees of freedom,  $k = m - n$ , is directly proportional to the variance,  $\text{VAR}[\chi_k^2] = 2k$ . If a system contains a large number of measurements,  $m$ , relative to the system states,  $n$ , the  $\chi^2$  test is poorly suited to detect bad data in the measurement set. A second weakness of the  $\chi^2$  test is that it is not able to identify what measurements contain bad data. Further analysis is required to be able to identify the bad data. A third weakness of the  $\chi^2$  test is the setting of the detection threshold. The number of false alarms is directly tied to the detection threshold [6].

### 3.4 Normalized Residuals Test

A second test for detecting bad data is the normalized residuals,  $r^N$ , test. For each measurement,  $i$ , the normalized residual is calculated from the gain matrix,  $G$ , and the measurement residuals,  $\hat{r}$ , by normalizing the residual by its estimated variance.

$$\begin{aligned} R_{\hat{x}} &= G^{-1} \\ R_{\hat{z}} &= HR_{\hat{x}}H^T \\ R_{\hat{r}} &= R_z - R_{\hat{z}} \\ &= SR_z \end{aligned} \tag{3.15}$$

$$\begin{aligned} \hat{r} &= z - \hat{z} \\ r_i^N &= \frac{\hat{r}_i}{\sqrt{R_{\hat{r}}(ii)}} \end{aligned} \tag{3.16}$$

The residual,  $\hat{r}$ , is defined by (3.11) and the residual covariance matrix,  $R_{\hat{r}}$ , by (3.13). Bad data can be detected in certain situations by comparing the normalized residuals to a defined threshold. In the presence of a single bad data, which is not a critical measurement, the largest normalized residual will correspond to the bad measurement [10]. Because the residual is normalized, the threshold is a multiple of the standard deviation, typically  $3\sigma$  or  $4\sigma$  [6]. If bad data is detected the measurement corresponding to the largest normalized residual can be removed and the WLS SE can be performed a second time [5]. It is possible to identify multiple bad measurements when the normalized residual exceeds a threshold for each measurement. But these measurement do not necessarily correspond to bad data because of a smearing effect on the measurement residuals [8].

An advantage of the normalized residual test over the  $\chi^2$  test is its ability to both detect and identify bad data. The largest normalized residual test will fail to detect bad data in critical measurements. Equation (3.15) shows that a critical (i.e. non-redundant) measurement will have a measurement residual covariance of zero. A critical measurement will have a variance equal to the variance of the measurement,  $R_z = R_{\hat{z}}$ , and the measurement estimate will equal the measured value,  $z = \hat{z}$  [3]. The  $\chi^2$  test is limited in its ability to detect bad data because it is based on (3.14), which uses the residuals as an approximation to the measurement errors [5]. Whereas normalized residuals provide a more accurate method of identifying bad data. The  $r^N$  test can further be improved upon by calculating an error estimate and correction factor for the measurement with the largest normalized residual.

### 3.5 Measurement Compensation And Normalized Residuals

The normalized residual test can be used to compensate measurements identified as bad data. One option in handling identified bad data is to remove it from the measurement set and re-run SE. This requires building the gain matrix a second time. A second option is to apply a correction factor to the bad measurement and continue with the current SE cycle [3]. The effect of measurement compensation is equivalent to eliminating the measurement from the measurement set. The advantage of this is that the measurement configuration is not changed. This eliminates the need to recalculate the gain matrix and does not change the measurement redundancy [12].

Assume that measurement  $j$  is identified as bad data. Then the residual estimate is given by

$$\hat{r} = S \cdot z$$

To minimize the effect of the bad data on the objective function, apply a correction



term,  $c_j$ , to the measurement, resulting in a new residual estimate.

$$\begin{aligned} z_j^{new} &= z_j + c_j \\ \hat{r}_j^{new} &= S_{jj} \cdot Z_j^{new} \\ &= S_{jj} \cdot (z_j + c_j) \end{aligned}$$

The effect of the bad data is minimized when the measurement residual is set to zero. The correction term is then defined by solving for  $c_j$ .

$$\begin{aligned} \hat{r}_j^{new} = 0 &= S_{jj} \cdot (z_j + c_j) \\ &= S_{jj} \cdot z_j + S_{jj} \cdot c_j \\ &= \hat{r}_j + S_{jj} \cdot c_j \\ c_j &= -\frac{\hat{r}_j}{S_{jj}} \end{aligned} \tag{3.17}$$

From the residual sensitivity matrix,  $S$ , defined by equation (3.11), the relationship between the correction term,  $c_j$ , and the error estimate,  $\hat{b}$ , is made (3.18).

$$\begin{aligned} c_j &= -\frac{\hat{r}_j}{S_{jj}} \\ S &= I - K \\ &= I - HG^{-1}H^T R_z^{-1} \\ &= (R_z - HG^{-1}H^T) \cdot R_z^{-1} \\ &= (R_z - R_{\hat{z}}) \cdot R_z^{-1} \\ &= R_{\hat{r}} \cdot R_z^{-1} \end{aligned}$$

For measurement  $j$ :

$$\begin{aligned} \sigma_j^2 &= R_z(jj) \\ S_{jj} &= \frac{R_{\hat{r}}(jj)}{\sigma_j^2} \\ c_j &= -\hat{r}_j \frac{\sigma_j^2}{R_{\hat{r}}(jj)} \\ &= -\sigma_j \cdot \hat{b}_j \end{aligned}$$

To implement measurement compensation after SE converges, the normalized residuals are calculated. The measurement corresponding to the largest normalized residual is suspected of having bad data and the correction term is calculated using equation (3.17). This correction term,  $c_j$ , is then applied to the measurement to obtain an estimate of the true measured value. Then an error estimate,  $\hat{b}_j$ , is calculated based on the measurement standard deviation,  $\sigma_j$ , measurement covariance,  $R_{\hat{r}}(jj)$ , and the normalized residual,  $r_j^N$ .

$$\hat{b}_j = \frac{\sigma_j}{R_{\hat{r}}(jj)} r_j^N \quad (3.18)$$

The error estimate is then compared to a chosen threshold to determine if the measurement is considered to be bad data. The threshold is set to a multiple of the measurement standard deviation ( $3\sigma_j$  or  $4\sigma_j$ ) [6].

### 3.6 3-Bus Example

A three-bus system is used to demonstrate the use of bad data processing in power system SE. The system includes a generating bus and two load buses connected by three lines, figure 3.3. The per-unit system parameters are given in table 3.1.

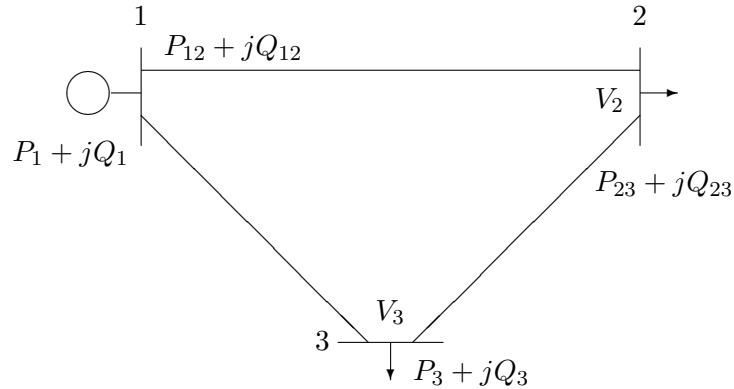


Figure 3.3: 3-Bus Example.

The example is set up by solving the power flow equations and then adding random Gaussian noise, mean of 0.0 and standard deviation of 0.01, to the calculated values to create the measurement set. A second measurement set with bad data is created by changing measurement  $P_{23}$  from 1.097 to 1.197. The measurement sets and corresponding objective function value are shown in table 3.2.

To apply the  $\chi^2$  test, five degrees of freedom are used (ten measurements minus five states). A confidence interval of 95% gives a  $\chi^2$  threshold of 11.07. This threshold value correctly identifies that bad data do not exist in the measurement set that results with an objective value of 3.9 and that bad data exist in the measurement set that results in an objective value of 85.0.

Table 3.3 gives the normalized residuals for this example. As expected, the largest normalized residual corresponds to the bad measurement. This demonstrates the advantage over the  $\chi^2$  test in that the  $r^N$  test is able to both detect and identify the bad data. With the bad data identified, it can simply be removed from the measurement set and SE can be resolved.

A weakness of the normalized residual test is seen in looking at the normalized residual for injection measurement  $P_3$  in table 3.3. The value of 8.78 is significantly greater than 3.0 or 4.0 but this measurement is not bad. The normalized residual is only able to detect one bad data at a time. When measurement  $P_{23}$  is removed SE converges with an objective value of 1.4, confirming that all bad data has been removed from the measurement set.

When measurement compensation is used instead of measurement removal, measurement  $P_{23}$  is corrected by subtracting an error value of 0.121, giving a measured value of 1.076. When SE converges the objective function is equal to 1.4, showing that the effect of the bad data has been removed.

line	R	X
1 to 2	0.015	0.020
1 to 3	0.060	0.150
2 to 3	0.010	0.030

Table 3.1: 3-Bus Example System Parameters.

Measurement	True Value	Measured	One Bad Data
$P_1$	2.089	2.083	2.083
$Q_1$	1.267	1.265	1.265
$P_{12}$	1.651	1.662	1.662
$Q_{12}$	0.949	0.425	0.425
$P_{23}$	1.097	1.097	<u>1.1974</u>
$Q_{23}$	0.577	0.568	0.568
$P_3$	-1.500	-1.478	-1.478
$Q_3$	-0.800	-0.799	-0.799
$V_2$	0.956	0.955	0.955
$V_3$	0.927	0.935	0.935
$J(x)$	1.5e-6	3.9	85.0

Table 3.2: 3-Bus Example.

	No Bad Data	Normalized Residual	One Bad Data	Normalized Residual
$P_1$	2.089	2.083	2.083	-0.98845
$Q_1$	1.267	1.265	1.265	-0.17789
$P_{12}$	1.651	1.662	1.662	2.08170
$Q_{12}$	0.949	0.425	0.425	-0.22592
$P_{23}$	1.097	1.097	<u>1.1974</u>	<u>9.16756</u>
$Q_{23}$	0.577	0.568	0.568	-0.77292
$P_3$	-1.500	-1.478	-1.478	8.78106
$Q_3$	-0.800	-0.799	-0.799	-0.72979
$V_2$	0.956	0.955	0.955	-0.50222
$V_3$	0.927	0.935	0.935	0.81117

Table 3.3: Normalized Residual Test Example.

### 3.7 Hypothesis Testing Identification Test

Hypothesis Testing Identification (HTI) is a method of identifying bad data in WLS SE that is based on estimating the measurement errors [10]. It is an improvement on the  $r^N$  test in that it is able to distinguish gross errors from good measurements that appear as bad data, and it is able to identify multiple bad data in a single SE cycle [14].

The effect of multiple conforming bad data can cause the residual of good measurement to be large [15]. The cause of this can be seen by looking at equations (3.9) and (3.11) which show that the measurement residual is the weighted sum of measurement errors. This occurred in the example in section 3.6. The normalized residual of measurement  $P_3$  was large due to the bad measurement  $P_{23}$ .

The HTI test expands on the  $r^N$  test by identifying suspect measurements and determining if each measurement contains bad data. The basis of the HTI method is that when no gross measurement errors exist in the measurement set then  $E[r] = 0$  and if bad data is present then  $E[r] \neq 0$ . A suspect measurement is identified as bad if its error estimate exceeds a threshold that is specific to each measurement. A measurement with a large normalized residual does not necessarily have a large error estimate.

A simple linear WLS example will be used to demonstrate the HTI method. Table 3.4 and figure 3.4 give the data and results. Each measurement has a standard deviation of 0.3 except measurement 7, which has a gross error of  $-4.78$ . The system is solved using WLS SE.

As expected, the largest normalized residual corresponds to measurement 7. The  $r^N$  test would correctly identify and remove measurement 7 as bad data. It is not able to test whether measurement 8 contains a gross error. One could remove all measurement above a given threshold (e.g. 3), but this would incorrectly identify measurement 8 as bad when it in fact is good, as shown in figure 3.4.

The HTI process is shown in figure 3.5. The method begins by identifying a set of suspect measurements. This set is reduced until all remaining measurements have been identified as bad data. The reduced set of bad measurements is then eliminated from the measurement set and the SE process continues.

After SE converges, the HTI process begins by calculating the residual sensitivity

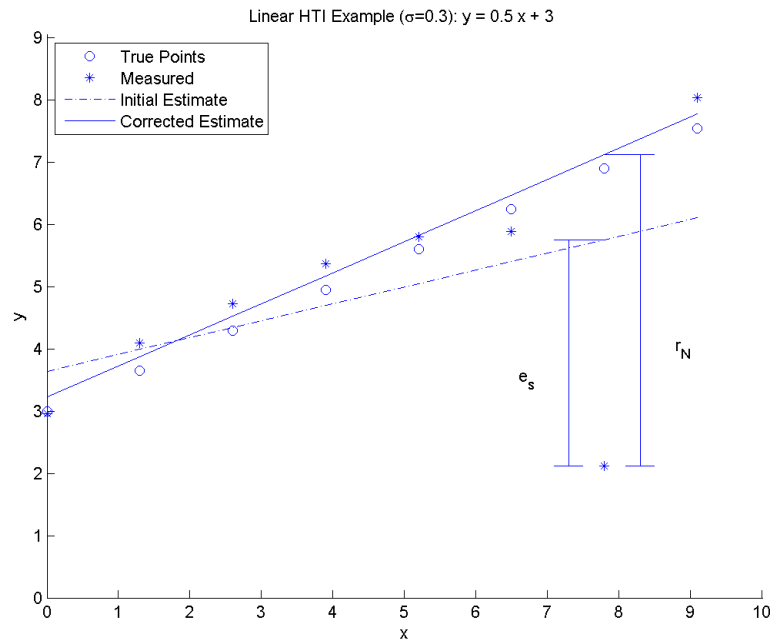


Figure 3.4: HTI Example.

x value	y true	y Measured	y Estimate	y Residual	y Normalized Residual	y Error Estimate
0	3.00	2.96	3.64	-0.68	-2.82	
1.3	3.65	4.10	4.00	0.10	0.38	
2.6	4.30	4.72	4.35	0.38	1.31	
3.9	4.95	5.38	4.70	0.68	2.30	
5.2	5.60	5.80	5.05	0.75	2.55	
6.5	6.25	5.89	5.40	0.49	1.69	
7.8	6.90	2.12	5.75	-3.64	<u>-13.51</u>	-4.7
9.1	7.55	8.04	6.11	1.93	8.01	0.6

Table 3.4: HTI Example Data.

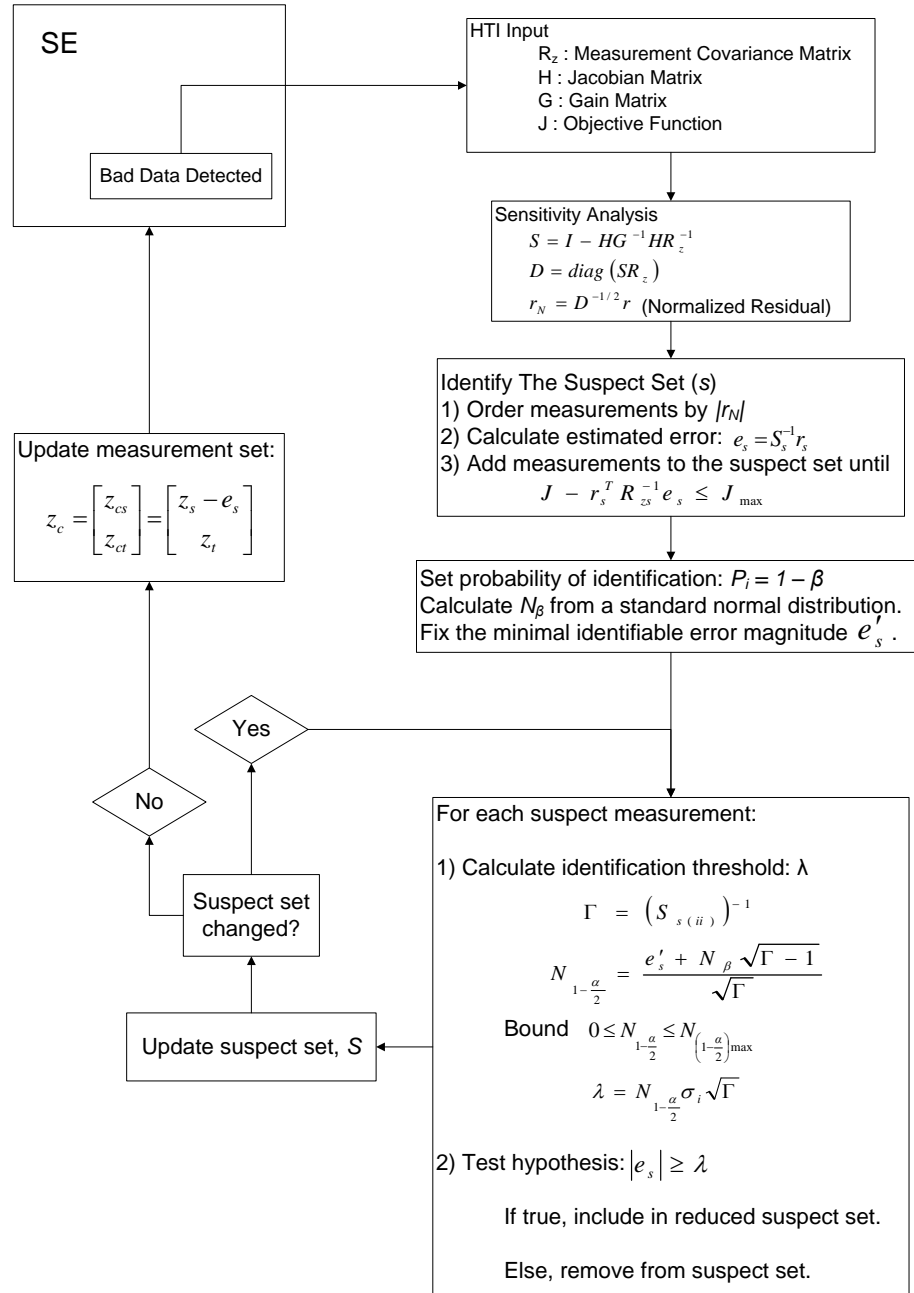


Figure 3.5: Hypothesis Test Identification Process.

matrix.

$$S = I - HG^{-1}H^T R_z^{-1} \quad (3.19)$$

When the measurement set is free of bad data, the measurement residual has a normal distribution with a variance of  $SR_z$  [10].

$$r \sim N(0, SR_z)$$

As a reference, figure 3.6 is a plot of a normal distribution with a mean of 0.0 and a standard deviation of 1.0. WLS SE is based on the assumption that the measurement errors follow a normal distribution with a mean of 0.0.

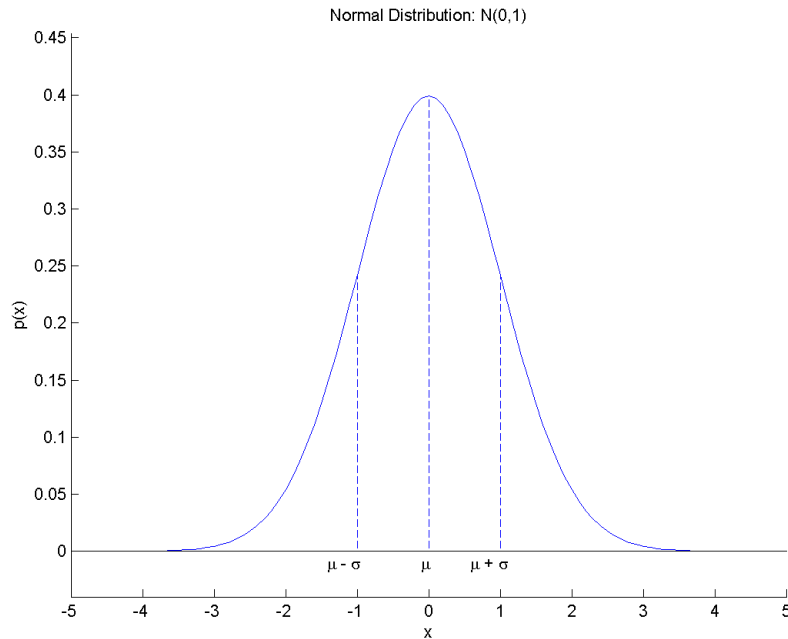


Figure 3.6: Normal Distribution Plot,  $N(0,1)$ .

Next, the normalized residual vector,  $r_N$ , is calculated from the measurement residual vector,  $r$ , the sensitivity matrix,  $S$ , and the measurement covariance matrix,  $R_z$ .

$$\begin{aligned} D &= \text{diag}(SR_z) \\ r_N &= \sqrt{D^{-1}} r \end{aligned}$$



To identify measurements suspect of bad data, the normalized residual vector is ordered by the absolute value. When a single gross error exists in the measurement set the largest normalized residual will correspond to this measurement [10]. If multiple bad data exist, it is assumed that it is likely that the largest normalized residual will correspond to the bad data [10]. This assumption is only used to build the suspect set and not to identify bad data. This prevents good measurements that appear as bad from being incorrectly identified as a bad measurement.

A suspect set of measurements is defined in one of two ways. One method is to include all measurements in the suspect set,  $s$ , with a normalized residual above a detection threshold. A second method is to add measurements to the suspect set until the objective function,  $J(x)$ , tests negative in the  $\chi^2$  test. The second method is preferred because the initial set of suspect measurements will be less than if the first method is applied. Also, an estimate of the objective function can be obtained without recalculating the state estimate by applying a correction factor to the current objective function value:

$$J(\hat{x}_c) = J(\hat{x}) - r_s^T R_{zs}^{-1} \hat{e}_s$$

$r_s$ : Residual vector of suspect measurements

$R_{zs}$ : Residual covariance matrix,  $R_z$ , of suspect measurements

$\hat{e}_s$ : Error estimate of suspect measurements

The process of adding measurements to the suspect set can be expanded upon to account for interacting measurements [14]. After the suspect set of measurements have been constructed, a test for measurement interaction can be performed. The correlation coefficient for each suspect measurement is calculated in the relation to the measurement with the largest normalized residual.

$$\rho_{ij} = \frac{\sigma_j S_{ij}}{\sigma_i \sqrt{S_{ii} S_{jj}}}$$

$\rho_{ij}$ : Correlation coefficient between measurement  $i$  and  $j$

$j$ : Measurement index corresponding to largest normalized residual

$i$ : Suspect measurement index,  $i \neq j$

If  $\rho_{ij}$  is less than a pre-defined tolerance, the measurement is included in the suspect set; otherwise, it is removed. The advantage of this is proper handling of interacting and non-interacting data. Interacting bad data should be handled separately to prevent the false identification of good measurements as bad. Non-interacting bad data can be handled in parallel to increase performance [14].

The next step is to calculate the error estimate for each suspect measurement. To do this the residual sensitivity matrix,  $S$ , and the residual vector,  $r$ , are reduced to the set of suspect measurements,  $s$ , and then used to calculate an error estimate:

$$\hat{e}_s = S_{ss}^{-1}r_s$$

With the estimated measurement error,  $\hat{e}_s$ , calculated the statistical properties of the measurement error estimates can be calculated.

$$\begin{aligned} E[\hat{e}_{s_i}|e_{s_i}] &= e_{s_i} \\ var[\hat{e}_s|e_s] &= \sigma_i^2(\Gamma_{ii} - 1) \\ \Gamma_{ii} &= (S_{ss})_{ii}^{-1} \end{aligned}$$

These quantities are shown in figure 3.7. The variance gives a measure of the precision of the error. The larger the variance the less precise or well known the measurement error is.

Next, a hypothesis test is performed to identify suspect measurements that are valid and those that are bad. First, define the hypothesis:

$$\begin{aligned} H_0: & \text{ the measurement is valid} \\ H_1: & \text{ the measurement is invalid} \end{aligned}$$

Hypothesis  $H_0$  corresponds with identifying the suspect measurement as free from bad data. Hypothesis  $H_1$  corresponds with identifying the suspect measurement as containing bad data. Figure 3.8 shows the essence of the hypothesis. The plot on the top shows the expected error distribution. The measurement error is near 2.5 standard deviations from the mean of 0. The point labeled  $e$  is the observed measurement error. The lower plot shows the possible error distribution if the measurement contains a gross error. The two plots in figure 3.8 show that as the magnitude of the observed error increases, the more likely the measurement contains a gross error.

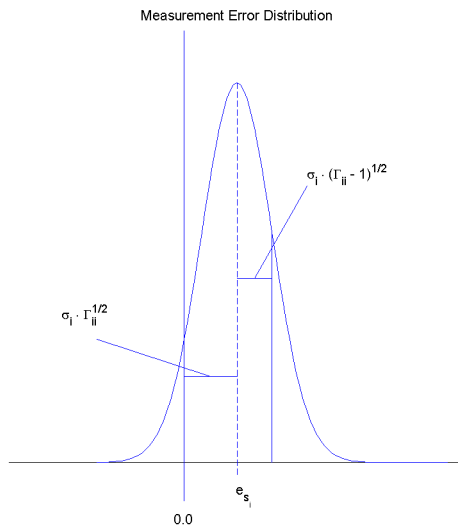


Figure 3.7: Measurement Error Distribution,  $N(e_{s_i}, \sigma_i^2(\Gamma_{ii} - 1))$ .

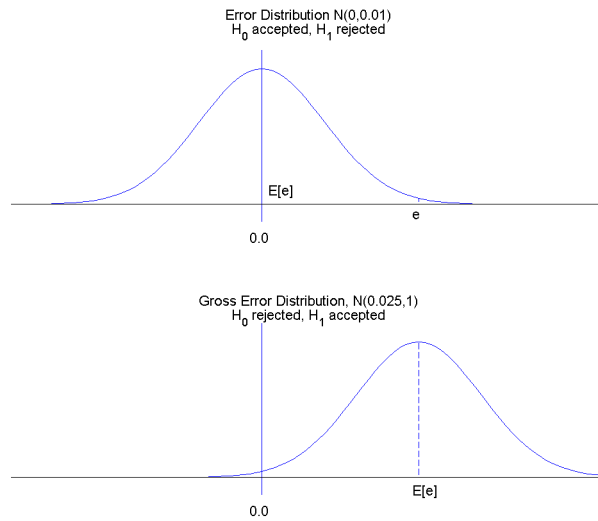


Figure 3.8: Error Distribution Plots,  $N(0,1)$ .

- $\alpha$ : Probability of rejecting  $H_0$  when  $H_0$  is true
- $\beta$ : Probability of rejecting  $H_1$  when  $H_1$  is true
- $P_i = 1 - \beta$ : Probability of identifying

The error probability  $\alpha$  is the probability of falsely identifying a good measurement as bad. The error probability  $\beta$  is the probability of failing to identify a bad measurement [10]. Figure 3.9 shows the relationship between the hypothesis test decision rules and the measurement error distribution.

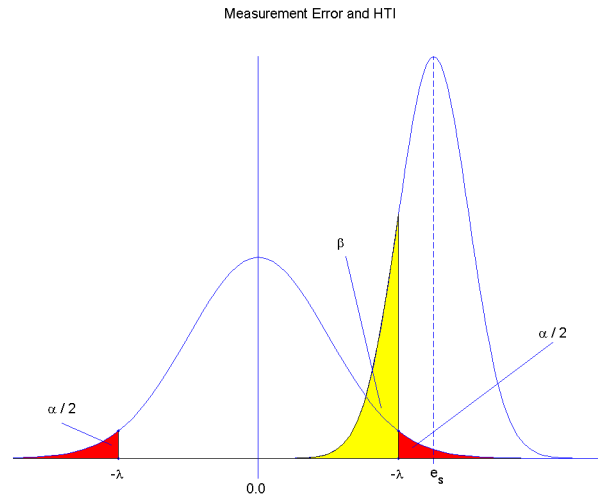


Figure 3.9: Error Distribution and Decision Rules.

To begin the hypothesis test, set the probability of identification,  $P_i = 1 - \beta$  (i.e.  $P_i = 99\%$ ). From this calculate the value of  $\beta$  from a normal distribution,  $N_\beta$ . This value of  $\beta$  and the probability of identification,  $P_i$ , stays fixed for all measurements. For each measurement calculate the identification threshold  $\lambda_i$ :

$$N_{1-\frac{\alpha}{2}} = \frac{e'_{s_i} + N_\beta \sqrt{\Gamma_{ii} - 1}}{\sqrt{\Gamma_{ii}}}$$

$$\lambda_i = N_{(1-\frac{\alpha}{2})_i} \sigma_i \sqrt{\Gamma_{ii}}$$

In this equation, the value of  $e'_{s_i}$  is fixed to a chosen value, e.g. 40. The value of  $N_{1-\frac{\alpha}{2}}$

is bound to prevent large values.

$$0 \leq N_{(1-\frac{\alpha}{2})_i} \leq N_{(1-\frac{\alpha}{2})_{max}}$$

Test each measurement error,  $e_{s_i}$ , against the corresponding threshold,  $\lambda_i$ .

$|e_{s_i}| > \lambda_i$ : Include measurement in reduced suspect set,  $S_2$ .

$|e_{s_i}| \leq \lambda_i$ : Remove measurement from the suspect set.

The process of reducing the suspect set stops once there is no change in the suspect measurement set. At this point all the remaining measurements in the suspect set have been identified as bad data.

Once a set of bad data are identified a correction factor, equation (3.20), can be applied to the measurement vector to obtain a corrected set of measurements. This is preferred over removing the bad measurements because it does not reduce the measurement redundancy. The effect of applying a correction factor is equivalent to removing the suspect measurements from the measurement set [10].

$$z_c = \begin{bmatrix} z_{cs} \\ z_{ct} \end{bmatrix} = \begin{bmatrix} z_s - \hat{e}_s \\ z_t \end{bmatrix} \quad (3.20)$$

The subscript  $c$  refers to the corrected vector,  $s$  to the suspect vector and  $t$  to the true vector. The  $t$  elements in the measurement vector consists of the measurements that are assumed to be true, free of gross errors. With the measurement set corrected a new SE cycle can be performed. If bad data is detected on subsequent SE cycles the HTI process can be used to identify the bad measurements.

## Chapter 4

# Topology Error Processing

A fundamental assumption of power system SE is that the topology of the network is accurately known. When this assumption is invalid the SE result will not correspond to the true state of the network. A topology error is defined as any error in telemetered or manually entered data that results in an incorrect network model. Topology errors tend to be a relatively rare occurrence, but when they do occur they can have a significant impact on the SE solution [16]. The need for topology error processing was first proposed in 1980 [17]. Since this time numerous methods have been proposed to detect and identify topology errors.

### 4.1 Topology Error Causes

There are numerous causes of topology errors. A common cause is the constantly changing nature of power system due to normal operation and equipment maintenance changes. A second contributing factor is that not all switches are telemetered. An example is circuit breaker bypass switches that are used to keep equipment in service during circuit breaker maintenance. When a maintenance crew closes a bypass switch that is not telemetered and opens and removes a circuit breaker that is telemetered the equipment can be incorrectly modeled as disconnected [9]. Additional causes can be a failure of the switch telemetry and unreported switch changes during routine maintenance [5]. When a system is being brought on line for the first time the power system SE program is used to correct telemetry [9]. During this phase of implementing an EMS

the number of topology errors can be relatively large [18].

## 4.2 Topology Error Types

Topology errors can be generalized into two categories:

**Branch Status Error** - the incorrect inclusion or exclusion of a branch in the bus-branch model.

**Substation Configuration Error** - the incorrect bus modeling of a group of bus-sections by merging multiple buses into a single bus or splitting a single bus into multiple buses.<sup>1</sup>

A primary difference between branch status errors and substation configuration errors is that the former involves equipment with non-zero impedances and the latter involves switches that are zero-impedance branches. In standard WLS SE, zero-impedance branches are not included in the bus-branch models. This makes detecting and identifying substation configuration errors considerably more complicated than branch status errors.

An additional complexity in identifying substation configuration errors is that a given substation can have multiple configurations depending on the status of switching elements. A given substation busbar section can be either connected or disconnected resulting in numerous configurations. A common substation configuration is the breaker-and-a-half. In this configuration a pair of breakers must be opened to disconnect a branch or an injection. Figure 4.1 shows three of the valid configurations this substation can take. As the complexity of the substation configuration increases, so does the number of possible configurations. This makes the process of identifying substation topology errors difficult.

A further degree of complexity is introduced by SE modeling the system at the bus-branch level and not the bus-section level. Because of this, numerous different types of switching element statuses can result in the same bus-branch configuration. Figure 4.2 shows the possible ways to create substation configurations where branches 1 and 4 are connected and branches 2 and 3 are connected.

---

<sup>1</sup> A *substation* is a group of bus-sections that are interconnected by switching devices [5]. If all the switching devices are closed, a single electrical node exists at the substation [2, 16].

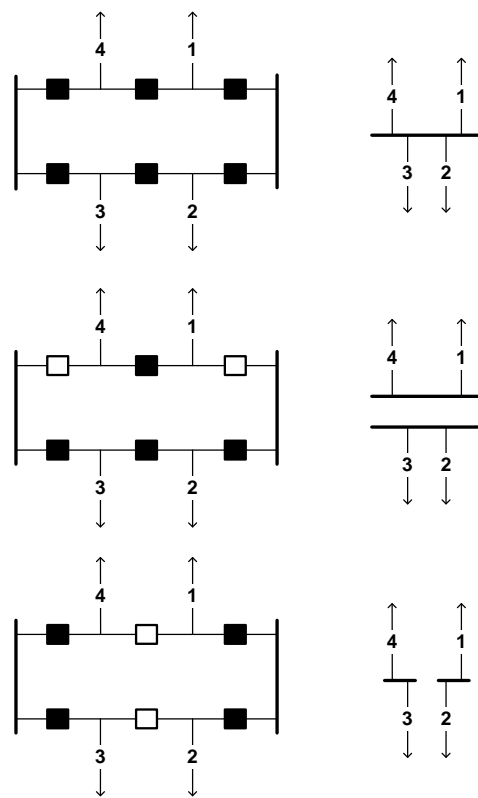


Figure 4.1: Breaker-And-A-Half Substation Configurations.



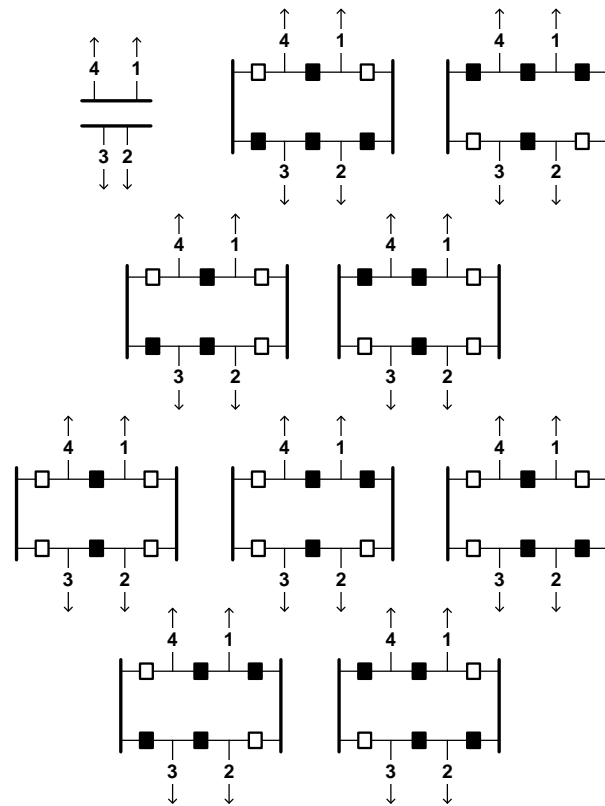


Figure 4.2: Breaker-And-A-Half Duplicate Substation Configurations.

Figure 4.3 gives examples of a branch status error and a substation configuration error. Table 4.1 gives the WLS SE solutions. In the first model, which is the true system, the location and type of measurements are shown. In the second model a branch exclusion topology error is shown. In the third model a bus-split topology error is shown. In the second and third models the normalized measurement residuals that exceed 3.0 standard deviations are shown.

The residuals in the vicinity of the topology errors have increased significantly (i.e. greater than 3 standard deviations) from the true system residuals. The two different topology errors cause varying effects on the residuals. The residuals of the bus split error are significantly larger than those due to the branch exclusion error. This intuitively makes sense because a bus split error can be viewed as multiple branch errors [19]. In the bus split topology error example the branches from bus 1 to 3 and 1 to 4 have been removed and branches 3 to 6 and 4 to 6 have been added relative to the true system.

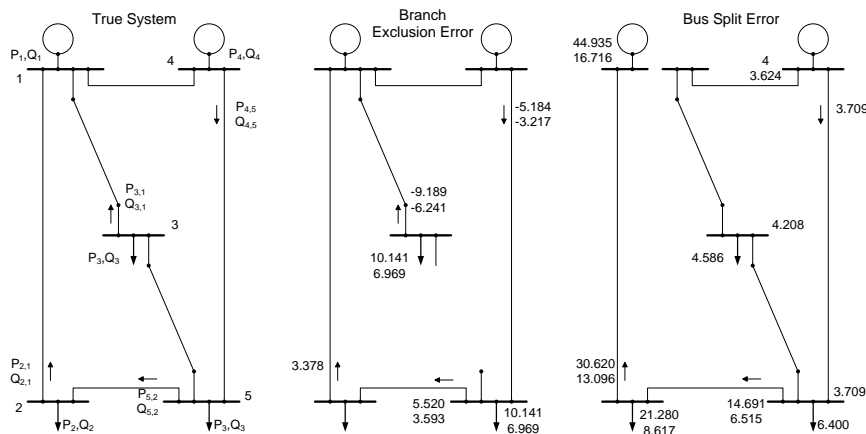


Figure 4.3: Topology Error Example.

### 4.3 Topology Error Effects

The effect of a topology error on the SE program can include divergence, false bad data detection, large measurement residuals and false or undetected limit violations [9]. Often a topology error results in multiple bad data in the vicinity of the topology error

Measurement		Estimated Value			Residual			Normalized Residual		
ID	Value	Base Case	Branch Exclusion	Bus Split	Base Case	Branch Exclusion	Bus Split	Base Case	Branch Exclusion	Bus Split
V1	1.000	1.000	1.003	1.011	0.000	-0.003	-0.011	0.029	-0.342	-1.257
V2	0.913	0.913	0.912	0.893	0.000	0.000	0.020	0.032	0.053	2.274
V3	0.928	0.928	0.940	0.891	0.000	-0.012	0.037	0.037	-1.358	4.208
V4	1.006	1.006	1.005	0.973	0.000	0.001	0.033	0.027	0.150	3.624
V5	0.911	0.911	0.905	0.878	0.000	0.006	0.033	0.035	0.697	3.709
P1	1.481	1.482	1.476	1.166	-0.001	0.005	0.316	-0.096	0.957	44.935
Q1	0.523	0.523	0.523	0.393	0.000	0.000	0.130	0.034	0.021	16.716
P2	-0.750	-0.750	-0.731	-0.894	0.000	-0.019	0.144	-0.026	-2.813	21.280
Q2	-0.250	-0.250	-0.239	-0.307	0.000	-0.011	0.057	-0.020	-1.710	8.617
P3	-0.500	-0.501	-0.578	-0.524	0.001	0.078	0.024	0.124	10.141	4.586
Q3	-0.100	-0.100	-0.153	-0.110	0.000	0.053	0.010	0.008	6.969	1.917
P4	1.000	1.000	1.003	1.003	0.000	-0.003	-0.003	-0.084	-0.460	-1.053
Q4	0.250	0.250	0.251	0.251	0.000	-0.001	-0.001	0.010	-0.133	-0.391
P5	-1.000	-1.000	-0.938	-1.032	0.000	-0.062	0.032	0.030	-8.827	6.400
Q5	-0.400	-0.400	-0.359	-0.412	0.000	-0.041	0.012	-0.032	-6.109	2.609
P2,1	-0.766	-0.766	-0.796	-1.018	0.000	0.030	0.252	0.001	3.378	30.620
Q2,1	-0.276	-0.276	-0.296	-0.378	0.000	0.020	0.102	-0.014	2.347	13.096
P5,2	-0.016	-0.016	-0.064	-0.121	0.000	0.048	0.106	0.021	5.520	14.691
Q5,2	-0.026	-0.026	-0.057	-0.071	0.000	0.032	0.045	0.001	3.593	6.515
P3,1	-0.648	-0.649	-0.578	-0.628	0.000	-0.071	-0.020	0.049	-9.189	-2.758
Q3,1	-0.200	-0.200	-0.153	-0.191	0.000	-0.047	-0.009	-0.005	-6.241	-1.208
P4,5	0.934	0.934	0.978	0.903	0.000	-0.045	0.030	-0.043	-5.184	3.709
Q4,5	0.284	0.283	0.312	0.270	0.000	-0.028	0.014	0.010	-3.217	1.635

Table 4.1: Topology Error Example State Estimator Values.

[20]. The influence of the topology error on the measurement residual is dependent on the system configuration, measurement redundancy and measurement location. The bad data processing in SE will remove these falsely identified measurements until the indication of bad data no longer exists [7]. This solution does not correspond to the true state of the system and fails to give an accurate system operating point to the system dispatcher.

#### 4.4 Topology Error Detection

The detection of topology errors is considerably more complex than that of measurement errors. The effect of a topology error is dependent on system configuration and measurement placement. In conventional power system SE, switches are not explicitly modeled and errors cannot be directly associated to the switches.

Some topology errors can be detected by comparing analog measurements and digital measurements. When a contradiction is found at a given equipment, the equipment can either be included or removed from the model to match the analog measurements. This type of topology error detection can be incorporated in the topology processor as a pre-processing step to SE. This can correct a large number of topology errors but does not account for equipment that does not have telemetry [9].

Extending bad data processing beyond measurement errors to include additional sources of errors tends to be difficult because these errors appear as analog measurement errors [21]. The correspondence between topology errors and measurement residuals is realized by looking at the linear measurement equation [19].

$$z = Hx + e$$

If a topology error exists then the Jacobian matrix,  $H$ , will contain errors.

$$H_t = H + H_e$$

$H_t$ : True measurement Jacobian matrix

$H$ : Calculated measurement Jacobian matrix

$H_e$ : Measurement Jacobian error matrix

The linearized relationship between the residuals and the measurements is given by

$$r = z - H\hat{x}$$

If the system contains a topology error, the residual will be affected by the topology error [5].<sup>2</sup>

$$\begin{aligned} r &= z - H\hat{x} \\ &= (I - K)(H_e x + e) \\ E(r) &= (I - K)H_e x \\ cov(r) &= (I - K)R \end{aligned} \tag{4.1}$$

If there is no topology error present in the system then  $H_e = 0$  and these equations reduce to those defined in section 3.2. Therefore, topology errors can be detected by residual analysis used in standard power system SE bad data processing.

The detectable conditions for a topology error can be determined from the expected values of the measurement residual, equation (4.1). A topology error is detectable if the expected value of the measurement residual is non-zero.

$$E(r) = (I - K)H_e x \neq 0$$

Certain topology errors can be undetectable due to a lack of measurements or negligible system flows and voltage differences [5]. The definition of a critical branch is necessary to define topology error detectable and identifiable conditions [22].

---

<sup>2</sup>

$$\begin{aligned} r &= z - H\hat{x} \\ &= z - H(G^{-1}H^T R_Z^{-1}z) \\ &= z - Kz \\ &= (H_t x + e) - K(H_t x + e) \\ &= (H_t x + e) - K(H_t x + e) + (Hx - Hx) \\ &= (H_t x + e) - K(H_t x + e) + (KHx - Hx) \\ &= [(H_t - H)x + e] - K[(H_t - H)x + e] \\ &= (H_e x + e) - K(H_e x + e) \\ &= (I - K)(H_e x + e) \end{aligned}$$

- Critical Branch: if removed makes the system unobservable
- Critical set of Branches: if the set is removed, the system becomes unobservable

A branch is not topology error detectable if it is a critical branch or incident only to critical measurements. A set of critical pair branches are topology error detectable but neither branch is topology error identifiable.

To determine which branches are topology error detectable and identifiable, take the matrix multiplication of the measurement-to-branch incidence matrix,  $M$ , and the residual sensitivity matrix,  $S$ . For each measurement  $i$ , the entry in  $M$  is defined as

$$M_{ij} = \begin{cases} 1 & \text{measurement } i \text{ at from side of branch } j \\ -1 & \text{measurement } i \text{ at to side of branch } j \\ 0 & \text{otherwise} \end{cases}$$

Let  $f_e$  be the vector of flow errors in the estimate due to the topology errors. Then the measurement residuals can be correlated to the branches.

$$\begin{aligned} H_e x &= M f_e \\ r &= (I - K)(M f_e + e) \end{aligned}$$

A branch is not topology error detectable if it corresponds to a zero column in the product of  $SM$  [22]. A set of two or more branches are not topology error identifiable if the set corresponds to a collinear set of columns [22].

## 4.5 Topology Error Processing Methods

A number of methods have been proposed to handle topology errors. One of the first methods proposed in [17] was a simple algorithm that looked at the measurement residuals to detect possible branch topology errors and subsequent SE runs to identify incorrect branch statuses. Other methods have ranged from geometric approaches in [22] to sensitivity analysis in order to identify incorrect branch statuses in [19]. Various methods based on Bayesian-based hypothesis testing have been proposed in [1, 23]. Two of the more commonly used methods are based on Generalized SE and Least Absolute Value SE. Both of these methods explicitly model switching elements and bus configurations in the model used by SE.

### 4.5.1 Generalized State Estimation

In conventional power system SE, the topology of the network and network parameters are assumed to be correct. The only bad data processing that occurs is for gross measurement errors. Generalized SE seeks to account for additional sources of errors by including parameters that are normally not estimated, including network parameters and system topology. The assumption that the correct network parameters and topology are known is no longer made in Generalized SE [7].

To include switching elements in Generalized SE, additional pseudo-measurements are added. For a closed switch the voltage drop across the switch is zero.

$$\begin{aligned} V_k - V_m &= 0 \\ \theta_k - \theta_m &= 0 \end{aligned}$$

For an open switch the power flowing through the switch is zero.

$$\begin{aligned} P_{km} &= 0 \\ Q_{km} &= 0 \end{aligned}$$

Explicit modeling of switching elements facilitates topology bad data processing by allowing direct topology processing by the SE program. A disadvantage is that the problem size grows drastically because the number of state variables and the number of pseudo measurements increases [18, 20]. Because the number of pseudo-measurements increase, the additional states created from the inclusion of a switch with a known status does not affect the system redundancy. But the inclusion of switches with an unknown state does reduce the measurement redundancy and can inhibit bad data processing [18]. Explicitly modeling switching elements also requires that the process of determining the observable portion of the network must be revised [20].

Observability analysis determines if the states of a power system can be determined from the measurement set [24]. This analysis confirms that the measurement model Jacobian matrix is full rank. Generalized SE requires that the classic methods of observability be reworked to account for the explicit modeling of switching elements, zero impedance branches, new state variables and power flows in switching elements [24].

### 4.5.2 Least Absolute Value State Estimation

Least Absolute Value (LAV) SE uses a two-stage process to detect and identify topological errors [25]. In the first stage, a state estimate is obtained from the bus-branch model and suspect measurements are identified. The suspect measurements are used to identify suspect buses that are modeled in detail in the second stage. This detail includes bus sections and switching elements. In the second stage only the suspect buses are modeled in detail to identify incorrect switching elements statuses. The correct position of switches is determined by calculating the flow through the switches. A primary advantage of the LAV estimator over the LS estimator is the ability to converge in the presence of bad data because of its robustness [25].<sup>3</sup>

The objective function of the weighted least absolute value (WLAV) estimator is

$$\min J(x) = \sum_{i=1}^m w_i |z_i - h_i(x)|$$

This can be converted to a linear programming (LP) problem

$$\begin{aligned} \min J(x) &= \sum_{i=1}^m w_i (u_i + v_i) \\ \text{s.t. } \Delta z^k &= H(x^k) \Delta x^k + u - v \end{aligned}$$

$z$ : vector of measurements, dimension  $m$

$h(x)$ : non-linear function relating measurements to the state vector

$x$ : state vector, dimension  $n$

$w_i$ : measurement  $i$  weight

$u, v$ : nonnegative slack variables

$u - v$ : measurement residual

$$\Delta z^k = z - h(x^k)$$

$$H(x^k) = \delta h / \delta x \text{ at } x^k$$

Additional constraints are added to indicate open and closed switching elements [5]. For a closed breaker  $i$  connected between nodes  $j$  and  $k$  the voltage drop is constrained to 0.

$$x_j - x_k + u_{m+i} - v_{m+i} = 0$$

---

<sup>3</sup> An estimators robustness is based on its ability to remain unbiased and reject outliers [5].



For an opened breaker  $i$  connected between nodes  $j$  and  $k$  the flow is constrained to 0.

$$f_{jk} + u_{m+i} - v_{m+i} = 0$$

The fact that the problem can be solved using a LP method is an advantage because there are well defined algorithms that can be used to solve the system, including the Simplex and Interior Point algorithms. A disadvantage with the LAV estimator is that its solution is less “optimal” than the WLS estimator. The WLS uses the complete set of measurements to estimate the states. Whereas the LAV estimator will satisfy  $n$  of  $m$  measurements where  $n$  is the number of states,  $m$  is the number of measurements and the system is fully observable [25].

Using either Generalized or Least Absolute Value SE for topology error processing is viewed as a weakness because these methods have not been widely used in EMS. Instead, a method of topology error processing using conventional Least Squares SE is sought. This is an advantage because of the primary use of the WLS SE in EMS.

## Chapter 5

# Topology Error Detection and Identification Using WLS State Estimation

A method of topology error detection and identification using the conventional WLS SE is proposed. Most of the methods of topology error processing require the reworking of conventional power system SE. The proposed method seeks to obtain the detection and identification of a topology error using conventional power system SE as detailed in chapter 2. The method is a post-processing addition to typical WLS SE that uses the SE results to detect topology errors and subsequent processing to identify the topology error. Figure 5.1 gives an overview of the process of detecting and identifying topology errors.

Power system SE has been used in EMS since the early 1980's. Since this time the WLS SE of power systems has been tested and improved upon to a high degree of reliability and accuracy. The presented method takes advantage of this fact by using the same WLS SE to detect and identify topology errors. Therefore, this method does not require the development or extension of power system SE to handle topology errors.

A two-stage approach is proposed. In the first stage, a standard WLS SE run is performed with bad data processing. The bad data processing results are used to detect suspect topology errors. The first stage ends with a list of equipment suspect of having

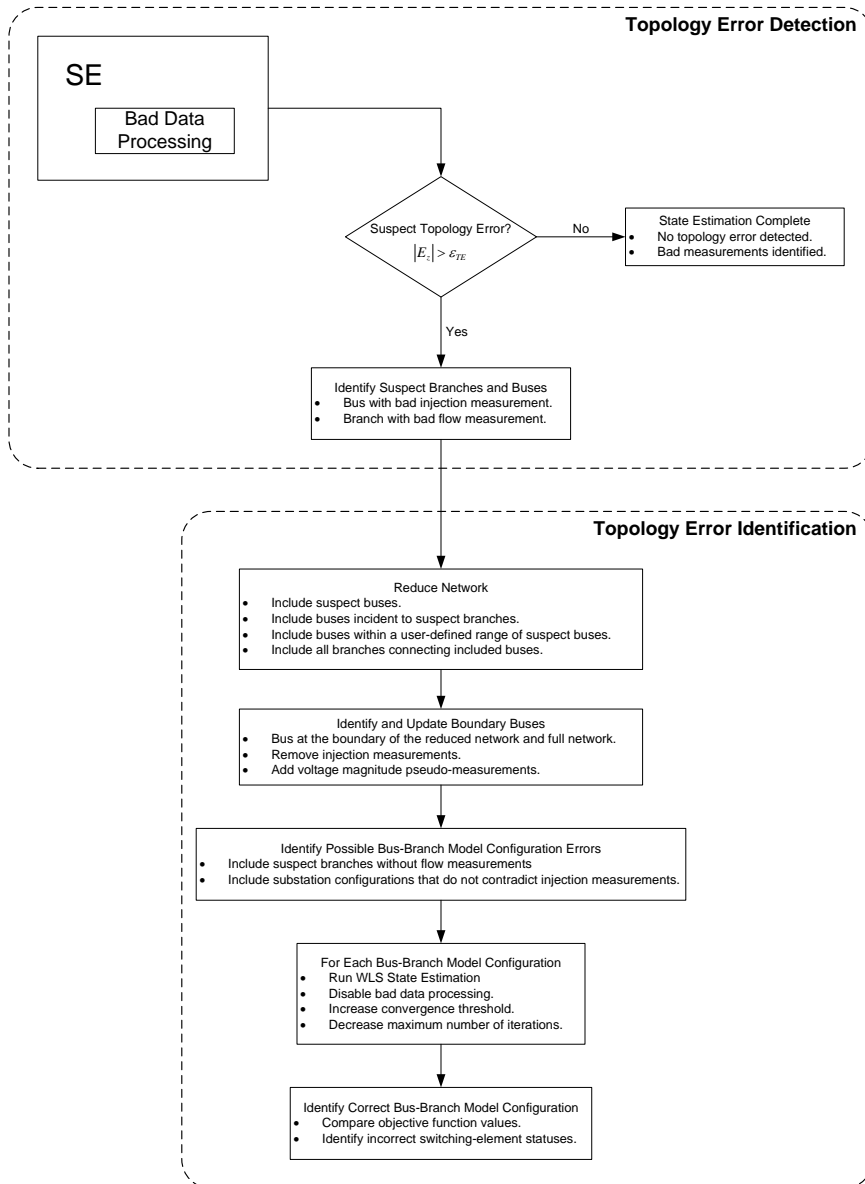


Figure 5.1: WLS Topology Error Identification And Detection.

a topology error. In the second stage, the topology errors are identified and the correct bus-branch model is determined. A two-stage approach is preferred for two reasons. First, power systems include vast networks that results in large models and data sets. Second, topology errors occur infrequently and in localized areas that do not affect the complete network. In spite of the infrequency, topology errors need to be addressed because of the significant impact they can have on the SE solution. The fact that topology errors rarely occur can be exploited by running the topology error processor as a second stage to conventional power system SE.

## 5.1 Stage One: Topology Error Detection

In stage one, WLS SE is performed with bad data processing to detect possible topology errors. As detailed in section 4.4, a topology error that is detectable results in increased measurement residuals in the vicinity of the topology error. A record is kept of each bad measurement, including the location and the normalized error magnitude. No additional computations are done during the SE process. When SE is completed, the magnitude of the error is compared against a user-defined threshold to determine if there is a suspect topology error at the associated equipment. The threshold used to identify suspect topology error is different than the threshold used to identify bad measurements in order to give the user the ability to adjust the sensitivity used in detecting topology errors separately than bad data. Often a topology error results in a measurement residual considerably larger than those due to bad measurement data. If there is no suspect topology error, SE is complete and no additional computations are done. If there are suspect topology errors, then additional analysis is done to identify the correct system topology. The first stage ends with a set of equipment suspect of having a topology error.

This approach requires minimal adjustments to the standard power system WLS SE. At this point, only minor additional processing is required to detect if a measurement exceeds an additional error threshold. At the end of this stage the SE results can be presented to the user and the additional functions included in the suite of transmission network applications that follow SE can be executed. If there is a suspect topology error detected, then additional processing can be done to either identify the topology

error or verify that the correct bus-branch model is being used.

## 5.2 Stage Two: Topology Error Identification

This stage begins with a set of equipment suspect of containing a topology error. The suspect set is used to identify the portion of the network in the vicinity of the suspect topology error that will be analyzed in detail for topology errors and to identify the correct bus-branch model. This stage will end with either identifying a topology error or verifying that the current system topology is valid. The criteria used to identify the correct bus-branch model is the WLS SE objective function.

### 5.2.1 Topology Error Identification Criteria

In a similar way that an optimal estimate of the operating state is obtained by minimizing the error between the measured and estimated values, it is sought to further minimize this objective value by adjusting the bus-branch model. It is assumed that the correct bus-branch model will result in the minimal possible objective function value. This is possible because a topology error is detectable due to its effect on the measurement residuals, section 4.4. This method seeks to identify the correct bus-branch model by identifying the topology adjustment that removes the increase in measurement residual due to the topology error.

One way to do this would be to obtain an SE solution for all possible switching element status combinations. Theoretically this would result in the correct system configuration. Practically this is impossible due to the number of combinations. This approach also is wasteful for a number of reasons. One, this would result in analyzing system configurations that are not feasible (e.g. system configurations with islands with no injections). Two, simulations would be run for systems with equipment statuses that contradict measurements (e.g. system configuration with a branch out of service that has a non-zero flow measurement). Three, multiple simulations would be run for the same bus-branch model. At a given substation, it takes multiple switching element status changes to split a substation into multiple buses. Lastly, this is not necessary because topology errors are infrequent. The proposed method seeks to exploit these points to use a recursive method to identify the correct system topology at the bus-branch level.

A topology error is identified by determining the correct bus-branch model. The correct bus-branch model is obtained by analyzing SE simulations for various bus-branch model configuration. Prior to each SE simulation, a check is performed to verify that the bus-branch model is valid. No radial buses with zero injections are simulated. No duplicate bus-branch model simulations are performed. No removal of branches with flow measurements are included. Once a topology error is identified, the operator can be notified to be able to verify the correct switch statuses.

### 5.2.2 Topology Error Identification Processing

The set of suspect equipment from stage one is now expanded to include incident equipment. This is done to account for variations in measurement location and redundancy. The expanded set is built by including the equipment associated with the measurements identified as bad. A bus with a bad injection measurement marks the bus and incident branches as suspect for a topology error. A branch with a bad flow measurement marks the branch and incident buses as suspect. This expansion includes all equipment independent of its status in the original model, allowing for the identification of branches that were incorrectly excluded from the original model. Branches with non-zero measurements are not included in this expansion process. It is assumed that the status of a branch with non-zero flow measurement is verified by its measurement.

Included in the identification stage is the reduction of the bus-branch model. The model is reduced to include the suspect equipment and the surrounding equipment. Suspect buses are marked as level one. The system is expanded to a level three. Level two buses are those that are connected to a level one bus by the distance of one branch. A level three is a single branch away from a level two bus.

#### Example of a Bus-Branch Model Reduction

Figure 5.2 gives an example of the substation levels for a suspect topology error at bus 18. In this example bus 18 and branches 30, 32 and 33 are suspect of topology errors. Buses 14, 16, 15, 17, 21 and 22 and branches 23, 24, 25, 26 and 28 are included in the reduced bus-branch model. Branches 19, 27 and 29 are removed from the reduced model. All measurements associated with equipment included in the reduced model at a level 1 and 2 are used. At level three, bus injection measurements are removed from buses

that are connected to a branch that is not included in the reduced model. The injection measurement at buses 14 and 16 have been removed, while the injection measurement at bus 22 is included. Voltage measurements at level three buses are included. If a level three bus does not have a voltage measurement, a pseudo-voltage measurement is used. This measurement is taken from the initial SE results. It is assumed that this measurement is sufficiently accurate because no bad data was incident to a level three bus. The purpose of removing the injection measurements at level three buses is to reduce boundary bus errors. These errors would result from the removal of branches at level three buses that do not connect to an included bus. This also allows for accurate estimation of the flows of branches connected between level two and level three buses. The effect of this is the same as modeling a branch as a bus injection.

### **Bus-Branch Model Topology Adjustments**

At this point, a set of equipment is identified as suspect for a topology error and the network model is reduced around this set of equipment. The next step is to identify the valid bus-branch model configurations. This can be split into two groups: branch status errors and bus-configuration errors. Each branch in the suspect set of equipment is analyzed to determine if it is correctly in or out of service. Each bus in the suspect set of equipment is analyzed to determine all valid bus configurations. A valid substation must have at least a branch and an injection or two branches.

### **State Estimation Topology Error Identification**

Next the set of suspect branches and buses are analyzed to determine the correct bus-branch model configuration. A SE simulation is performed for each possible bus-branch model configuration. A base case simulation is done on the reduced network. This provides a benchmark to determine if a topology error exists. Prior to running additional simulation on an alternative bus-branch model configuration, a check is done to verify that the current bus-branch model is different than all previously simulated bus-branch models. This check is done by creating a unique vector that identifies each simulated bus-branch model. The unique vector contains an ordered list of the from and to bus of each branch, the generator buses and injection buses. The purpose of this is to reduce the total number of simulations. For a suspect branch that was included in the base case,

only a single simulation is required to test if its correct status is out of service. This simulation includes removing the branch from the model and recording the resulting objective function value. The base case includes the simulation of the branch in service. Therefore, the number of required simulations for branches statuses is the number of suspect branches plus one for the base case. The number of simulations needed for a bus is dependent on the specific bus. The bus in figure 4.1 requires three simulations, one of these being included in the base case.

In each SE simulation limited bad data processing is performed. The bad data processing is limited to measurement removal instead of measurement correction. It is possible to obtain a minimum objective value for an incorrect topology configuration when measurement correction is used in the bad data processing. Measurement correction in the vicinity of a topology error results in conforming the measurements to the topology error. To prevent this, only measurement removal is used.

At the completion of each SE simulation, a record is kept of the objective function value. When all simulations have completed the correct bus-branch model is identified by the SE simulation with the minimum objective value. At this point, the user is presented the identified topology error and the objective value. This objective value can be used to verify the likeliness of this bus-branch model and associated topology error.



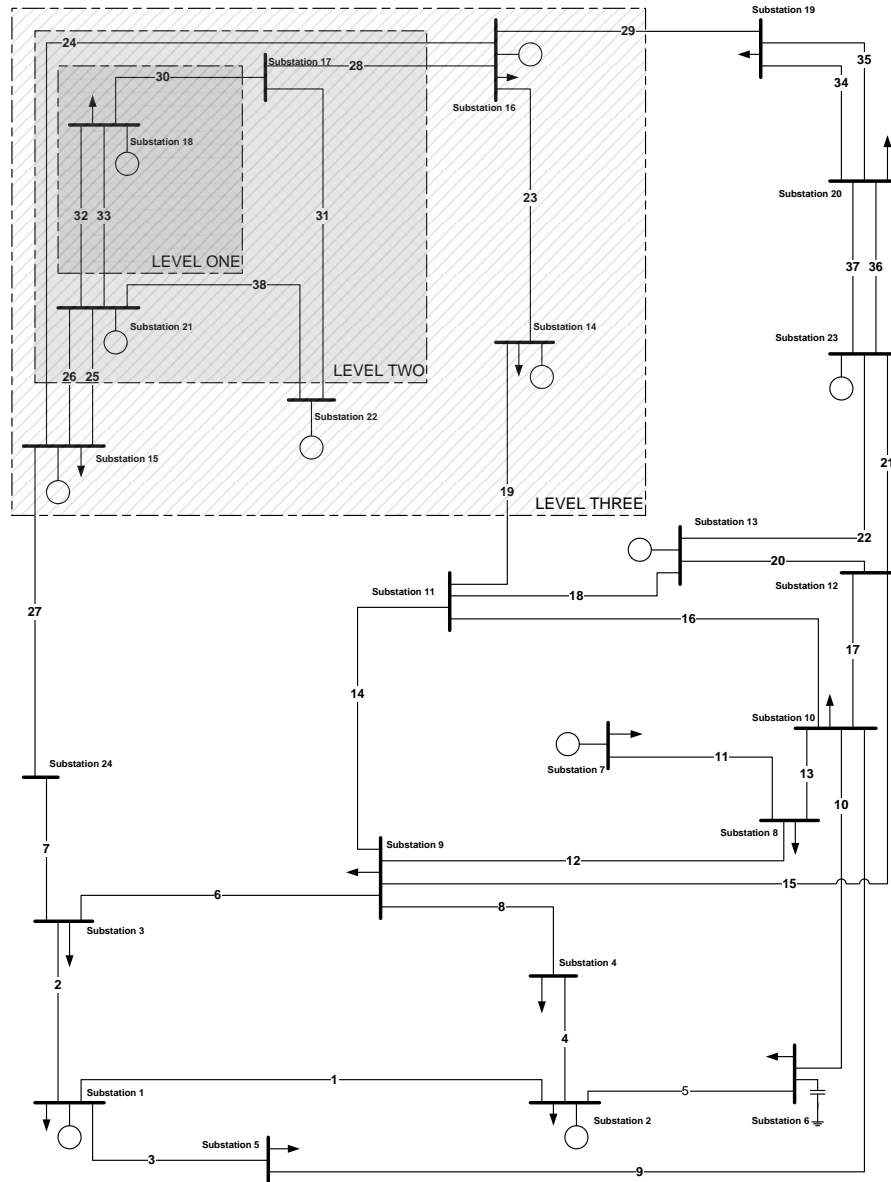


Figure 5.2: Bus-Branch Model Inclusion Levels.

## Chapter 6

# Topology Error Detection and Identification: MATLAB Simulation

The method of detecting and identifying topology errors, detailed in chapter 5, has been implemented in MATLAB. The MATLAB program includes WLS SE, a topology error processor and an interface with MATPOWER, a power flow (PF) program. The PF program is used to produce measurements for SE. The test system is the 24-bus model of the IEEE Reliability Test System [26]. Figure 6.1 gives an overview of the research implemented in MATLAB. The IEEE Reliability Test System provides the input data. The MATPOWER power flow obtains a system operating point. The SE program determines the optimal estimate of the system. The topology error processor detects and identifies topology errors.

### 6.1 MATPOWER

A power flow simulation is needed to obtain a system operating point of the model from which SE measurements can be created. MATPOWER is an open-source power system simulation package primarily used in optimal PF research and education [27]. In this research, MATPOWER is strictly used to obtain a system operating point and to

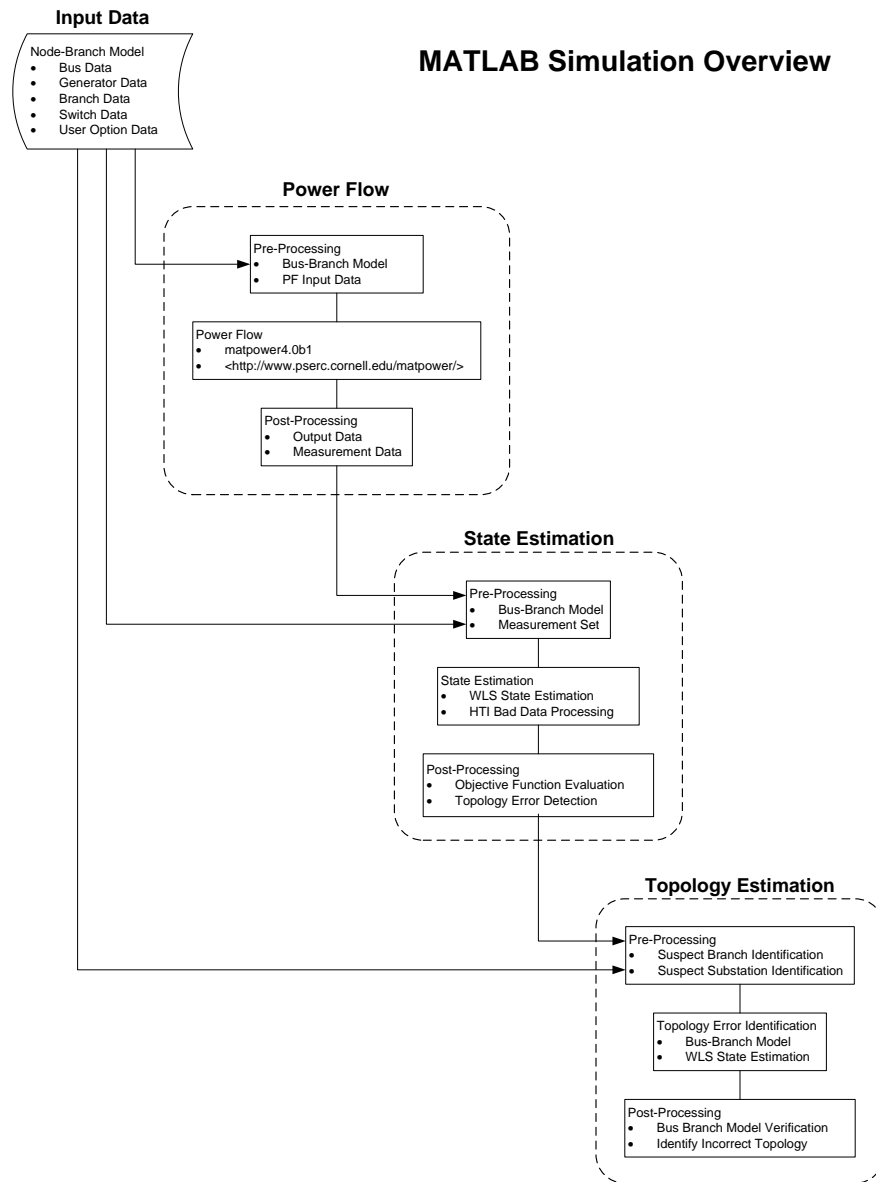


Figure 6.1: MATLAB Program Overview.

produce SE measurements. The output of the PF solution is used to create bus voltage magnitude, bus injection and branch flow measurements. Noise is added to the values to produce realistic measurements. MATLAB's normally distributed random number generator, RANDN, is used to produce the noise [28]. Gross measurement errors can be defined by the user in multiples of the measurement standard deviations. The purpose of this is to test the ability of the topology error processor to detect and identify topology errors in the presence of bad data.

A secondary benefit of using MATPOWER is to verify the SE solution. In the case that no noise is added to the measurement set, the SE solution solves to a near-zero objective function value and system values match the power flow solution. When changes are made to the SE program, the correctness and accuracy of these changes can be verified by comparing the SE solution to the PF solution.

## 6.2 WLS State Estimator

WLS SE algorithm along with bad data processing was implemented in MATLAB, as detailed in chapter 2. The iterative solution is obtained by using MATLAB's matrix divider, MLDIVIDE. MATLAB's function, MLDIVIDE, gives the least squares solution to  $Ax = B$ . This MATLAB function uses QR decomposition with column pivoting to obtain a minimum of the length of the vector  $Ax - B$  [29]. Three types of bad data processing were implemented: Largest Normalized Residual (LNR) with measurement removal, Largest Normalized Residual with measurement correction and Hypothesis Test and Identification (HTI). It is possible to use each of these methods to identify possible topology errors. This research uses the HTI method of bad data processing to detect possible topology errors. The HTI method was chosen for its ability to detect multiple bad data in a single SE cycle. This is an advantage in detecting topology errors because a single topology error often results in multiple measurements being identified as bad data.

### 6.3 24-Bus IEEE Reliability Test System

The IEEE Reliability Test System was developed to test methods for reliability analysis of power systems and provide a basis of comparison of results [26]. The system was developed by the IEEE Subcommittee on the Application of Probability Methods. The model contains 32 generating units, 24 substations and 38 connecting branches. It also has two voltage corrective devices; at bus 14 there is a synchronous condenser and at bus 6 there is a reactor. Figure 6.2 shows the bus-branch model of the system. This system was enhanced in [30] to give a more complete data set to insure consistency in system testing. A full set of switching configurations was added in [31]. Recently a three-phase breaker-oriented model of the 24 substation Reliability Test System was developed in [32].

The IEEE Reliability Test System was chosen because of its acceptance and use as a benchmark in testing power system analysis methods [32]. Since it was first developed it has been used to test advanced power system analysis algorithms. It was also chosen because of the full switch-oriented model that was developed in [33]. As noted in [32], a full switch-oriented model is needed to analyze topology estimation in the context of SE. Figure 6.3 shows the bus-section model used in this research, which is based on the model in [33].

### 6.4 Topology Error Test Cases

Four types of topology errors are presented as test cases. These four examples include the most common topology errors: branch exclusion, branch inclusion, bus split and bus merge. In each case a power solution is obtained to provide a valid operating point for the specific configuration. A complete measurement set is used to give the most detail on the effect of a topology error on measurement residuals. The complete measurement set includes bus real and reactive injections, bus voltage magnitudes and branch real and reactive flows at the *from* and *to* end. A zero-injection pseudo-measurement is added at each bus that does not contain any generation or load. Each measurement is created by adding normally distributed random noise with a standard deviation of 0.01 to each measurement.

As a benchmark, figure 6.5 gives the base case MATPOWER PF solution and the

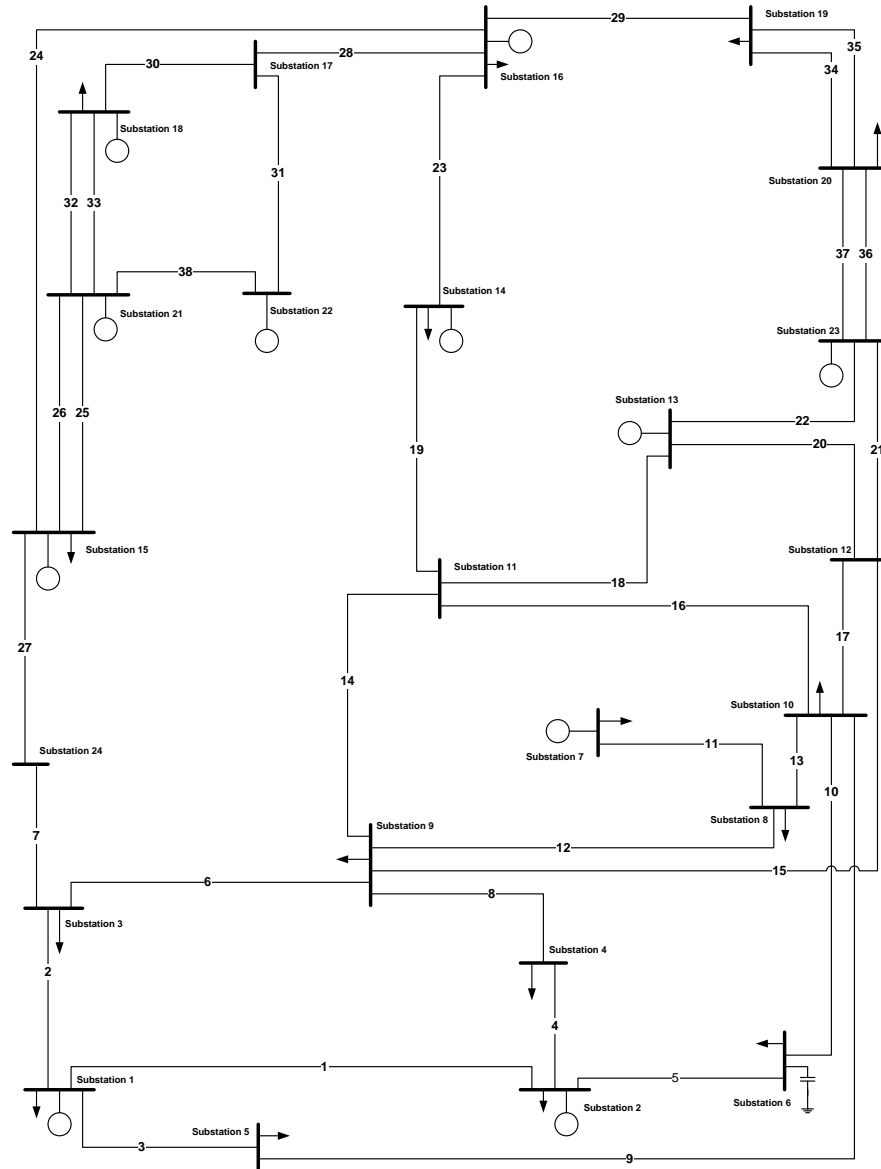


Figure 6.2: IEEE Reliability Test System.

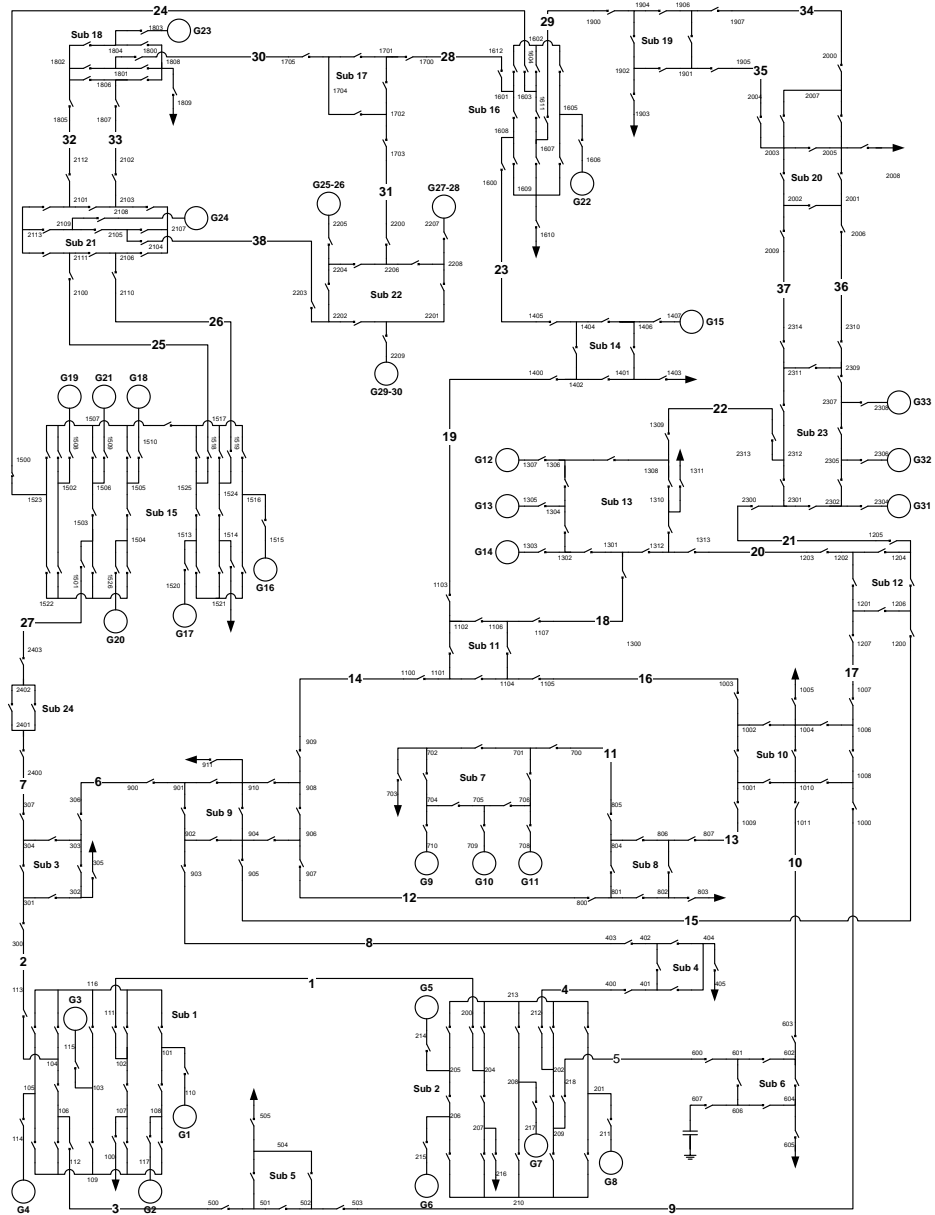


Figure 6.3: IEEE Reliability Test System: Switch-Oriented Model.

SE solution. SE converged in 5 iterations with an object value of 180.0 and no bad data detected. The SE solution is slightly different than the PF solution but within the range of the standard deviations of the measurements.

#### 6.4.1 Branch Exclusion

A branch exclusion error is a topology error of excluding a branch in the bus-branch model when it is in-service in the physical system. To simulate this error, branch 14, from bus 9 to bus 11, is removed from the model used by SE and included in the model used by the power flow program. Figure 6.6 gives the PF and SE solution. SE converged in 29 iterations with an objective function value of 324.96 and 31 measurements were identified as bad, table 6.7. As expected, these measurements are in the vicinity of the excluded branch 14. Table 6.1 lists the substations and branches identified as suspect for a topology error. The topology error processor identifies that branch 14 was incorrectly modeled as out of service.

Station Number	Branch Number	From Bus	To Bus
3	14	900	1105
4			
8			
9			
11			
12			
13			
14			

Table 6.1: Branch Exclusion Suspect Equipment.

#### 6.4.2 Branch Inclusion

A branch inclusion error is a topology error of including a branch in the bus-branch model when it is out-of-service in the physical system. The same branch used in the branch exclusion error example is used. To simulate this error, branch 14 from bus 9 to bus 11 is included in the model used by SE and removed from the model used by



the power flow program. Figure 6.7 give the solution for PF and SE. SE converged in 33 iterations with an objective function value of 268.92 and 70 measurements were identified as bad, table 6.8. Table 6.2 lists the substations and branches identified as suspect for a topology error. The topology error processor identifies that branch 9 was incorrectly modeled as in service.

Station Number	Branch Number	From Bus	To Bus
3	14	900	1100
4			
8			
9			
10			
11			
12			
13			
14			
16			
23			

Table 6.2: Branch Inclusion Suspect Equipment.

### 6.4.3 Bus Merge

A bus merge topology error is the incorrect modeling of a substation bus as one electrical bus when it is two buses in the physical system. Bus 9 is merged into a single bus from a split bus in the PF solution. Figure 6.8 gives the solution for PF and SE. SE converged in 45 iterations with an objective function value of 321.71 and 96 measurements were identified as bad, table 6.9. Some of these measurements were identified multiple times as bad data. The cause of this is the interaction of the topology error and the measurement correction that is used on the bad data. Table 6.3 lists the substations identified as suspect for a topology error. The topology error processor identifies that substation 14 was incorrectly modeled as two buses.

#### 6.4.4 Bus Split

A bus split topology error is the incorrect modeling of a substation bus as two electrical buses when it is one bus in the physical system. A bus split topology error is simulated by splitting bus 9 in the SE model and not in the PF model. Bus 9 is split into two buses as shown in figure 6.4. Figure 6.9 gives the solution for PF and SE. SE converged in 7 iterations with an objective function value of 165.13 and two measurements were identified as bad, table 6.10. Table 6.4 lists the substation identified as suspect for a topology error. The topology error processor identifies that substation 9 was incorrectly modeled as a single bus.

#### 6.4.5 Measurement Location and Topology Error

The bus split topology error in section 6.4.4 can be used to show the importance of measurement location. If the injection measurements at both of the bus sections at substation 9 are removed, the topology error is no longer detectable. Figure 6.11 gives the PF and SE solution. The effect of the bus split topology error is sufficiently small to not create any measurement errors. The max normalized measurement residual is  $-2.2$  on the reactive flow of branch 4 between substations 2 and 4. This is below the typical threshold of 3.0 standard deviations. If one compares the SE solution to the system model in figure 6.4, it is clear that this is not a valid solution because there is no load at substation bus  $9b$ , bus 907 in figure 6.11.

One way to make this topology error detectable is to add a zero-injection pseudo-measurement at substation bus labeled  $9b$  in figure 6.4. The effect of adding this measurement is the detection and identification of the bus split topology error. The zero-injection measurement is flagged as bad, initiating the topology error processor.

This example shows the importance of both measurement location and the use of zero-injection pseudo-measurements to be able to detect and identify topology errors. A zero-injection measurement acts as a constraint in SE by requiring that the estimated solution matches the physical system.

Station Number
8
9
10
11
12
14
16
23

Table 6.3: Bus Merge Suspect Equipment.

Station Number
3
4
8
9
11
12

Table 6.4: Bus Split Suspect Equipment.

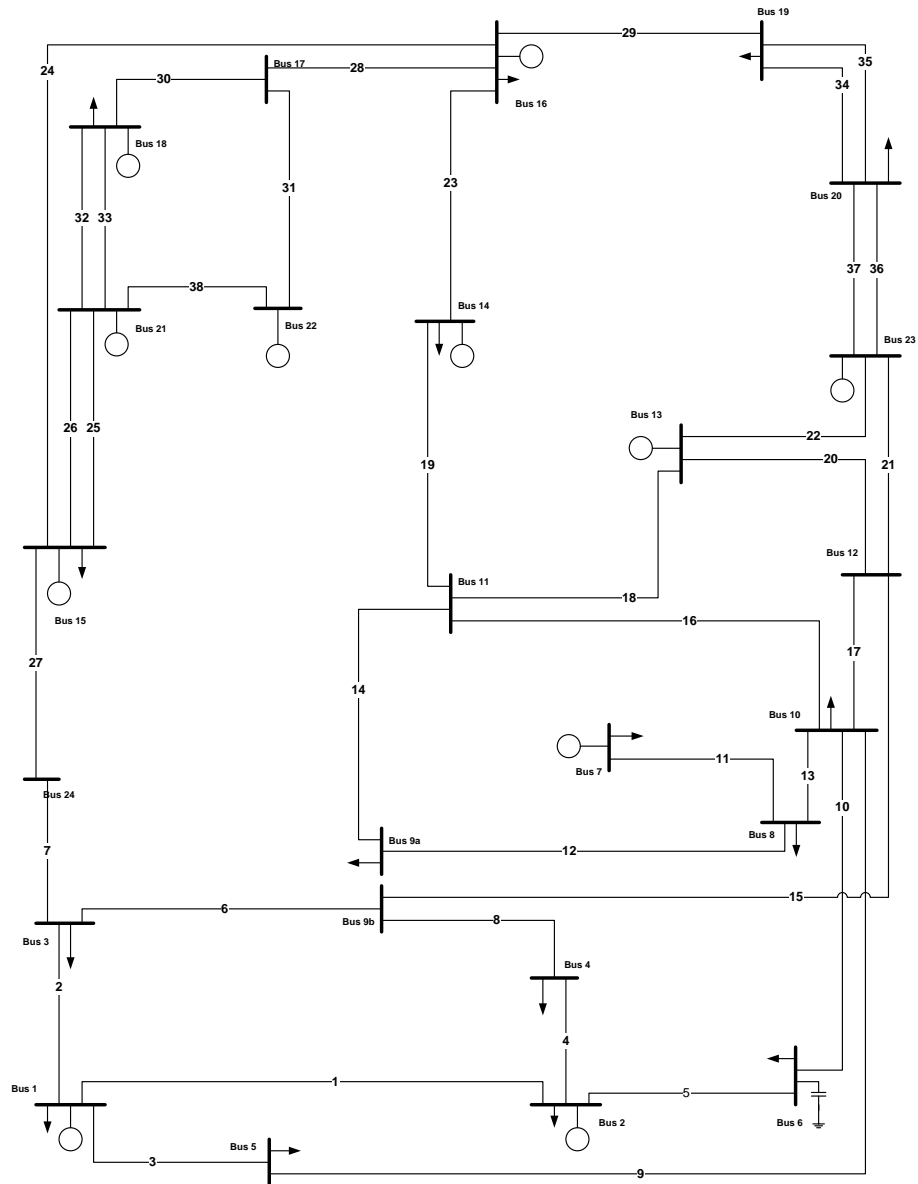


Figure 6.4: Bus 9 Split Example.

### 6.4.6 Bad Measurement Data and Topology Error

As discussed in chapter 3, bad data processing is an essential component of SE. The process of detecting and identifying topology errors must work in the presence of bad data. An extreme case of bad data is the reverse connection of a measuring device, resulting in the negative of the true value. To simulate this type of bad data along with a topology error, branch 14 has been removed from the PF model and included in the SE model as in the example of section 6.4.1. In addition, a gross measurement error was added to the flow on branch 18, from substation 11 to 13, table 6.5.

Measurement ID	True Value (pu)	Gross Error (pu)	Measured Value (pu)
PF 1105, 1300	-0.5787	+0.117	0.5913
QF 1105, 1300	-0.0886	+0.170	0.0814

Table 6.5: Bad Measurement Data On Branch 18.

Station Number	Branch Number	From Bus	To Bus
10	14	900	1100
11			
13			
14			
16			

Table 6.6: Bad Data And Topology Error Suspect Equipment.

Figure 6.10 gives the PF and SE solution and table 6.11 gives the measurements identified as bad in SE. SE identifies the gross measurement errors but applies an invalid correction due to the topology error, table 6.11. SE converged to a solution and identified equipment as suspect for a topology error table 6.6. From the set of suspect equipment, the topology error processor correctly identified the topology error as the incorrect inclusion of branch 14 in the SE bus-branch model. This example shows the ability of this method to detect a topology error in the presence of bad data.

MATPOWER PF SOLUTION						SE SOLUTION									
BUS	VOLTAGE	ANGLE	Pinj	Qinj	To Bus	Plane	Qline	BUS	VOLTAGE	ANGLE	Pinj	Qinj	To Bus	Plane	Qline
100	1.050	0.000	0.760	-0.052	200	0.102	-0.273	100	1.049	0.000	0.758	-0.040	200	0.106	-0.263
					300	-0.002	0.211						300	-0.003	0.213
					500	0.660	0.010						500	0.655	0.010
200	1.050	-0.077	0.870	-0.085	100	-0.102	-0.235	200	1.049	-0.078	0.865	-0.092	100	-0.106	-0.245
					400	0.446	0.189						400	0.446	0.191
					600	0.526	-0.038						600	0.525	-0.038
300	1.001	0.745	-1.800	-0.370	100	0.005	-0.260	300	1.000	0.766	-1.792	-0.364	100	0.006	-0.261
					900	0.208	-0.175						900	0.212	-0.172
					2400	-2.012	0.065						2400	-2.011	0.069
400	1.012	-2.759	-0.740	-0.150	200	-0.439	-0.197	400	1.011	-2.764	-0.738	-0.149	200	-0.439	-0.199
					900	-0.301	0.047						900	-0.299	0.050
500	1.036	-2.911	-0.710	-0.140	100	-0.651	-0.002	500	1.035	-2.893	-0.704	-0.136	100	-0.646	-0.002
					1000	-0.059	-0.138						1000	-0.058	-0.133
					SHUNT: -1.064								SHUNT: -1.062		
600	1.031	-5.454	-1.360	-0.280	200	-0.514	0.030	600	1.031	-5.452	-1.361	-0.274	200	-0.512	0.030
					1000	-0.846	-1.374						1000	-0.849	-1.367
700	1.045	-3.130	0.875	0.348	800	0.875	0.348	700	1.043	-3.123	0.871	0.340	800	0.871	0.340
800	1.012	-5.734	-1.710	-0.350	700	-0.862	-0.315	800	1.010	-5.733	-1.706	-0.346	700	-0.859	-0.308
					900	-0.487	0.108						900	-0.485	0.107
					1000	-0.361	-0.143						1000	-0.363	-0.145
900	1.014	-0.924	-1.750	-0.360	300	-0.205	0.150	900	1.013	-0.935	-1.763	-0.363	300	-0.210	0.147
					400	0.303	-0.067						400	0.301	-0.069
					800	0.498	-0.113						800	0.495	-0.112
					1100	-1.100	-0.210						1100	-1.100	-0.209
					1200	-1.246	-0.121						1200	-1.248	-0.120
1000	1.048	-2.787	-1.950	-0.400	500	0.059	0.114	1000	1.047	-2.768	-1.936	-0.398	500	0.058	0.109
					600	0.856	-1.243						600	0.858	-1.245
					800	0.367	0.119						800	0.369	0.122
					1100	-1.542	0.256						1100	-1.536	0.260
					1200	-1.690	0.353						1200	-1.686	0.357
1100	1.038	4.077	-0.000	-0.000	900	1.103	0.312	1100	1.037	4.082	-0.000	0.000	900	1.103	0.312
					1000	1.547	-0.070						1000	1.541	-0.074
					1300	-1.019	-0.161						1300	-1.020	-0.162
					1400	-1.631	-0.082						1400	-1.624	-0.075
1200	1.032	4.790	-0.000	-0.000	900	1.249	0.248	1200	1.031	4.807	-0.000	0.000	900	1.252	0.249
					1000	1.696	-0.126						1000	1.692	-0.130
					1300	-0.751	-0.331						1300	-0.749	-0.333
					2300	-2.194	0.208						2300	-2.195	0.213
1300	1.050	6.592	-0.308	0.699	1100	1.025	0.098	1300	1.049	6.607	-0.311	0.710	1100	1.026	0.100
					1200	0.755	0.252						1200	0.753	0.253
					2300	-2.087	0.349						2300	-2.090	0.356
1400	1.050	7.654	-1.940	0.807	1100	1.645	0.089	1400	1.048	7.656	-1.955	0.799	1100	1.637	0.082
					1600	-3.585	0.718						1600	-3.592	0.717
1500	1.044	15.922	-1.500	0.460	1600	0.828	-0.332	1500	1.043	15.971	-1.485	0.464	1600	0.835	-0.326
					2100	-2.188	0.212						2100	-2.184	0.213
					2100	-2.188	0.212						2100	-2.184	0.213
					2400	2.049	0.367						2400	2.047	0.364
1600	1.048	15.136	0.550	0.600	1400	3.646	-0.334	1600	1.046	15.177	0.551	0.597	1400	3.654	-0.329
					1500	-0.826	0.304						1500	-0.834	0.299
					1700	-3.155	0.455						1700	-3.151	0.454
					1900	0.886	0.174						1900	0.882	0.173
1700	1.049	19.484	-0.000	-0.000	1600	3.185	-0.275	1700	1.047	19.533	0.000	0.000	1600	3.181	-0.273
					1800	-1.799	0.135						1800	-1.795	0.134
					2200	-1.386	0.140						2200	-1.386	0.140
1800	1.050	20.847	0.670	-0.033	1700	1.804	-0.125	1800	1.048	20.896	0.662	-0.033	1700	1.801	-0.124
					2100	-0.567	0.046						2100	-0.570	0.046
					2100	-0.567	0.046						2100	-0.570	0.046
1900	1.041	14.093	-1.810	-0.370	1600	-0.883	-0.210	1900	1.039	14.135	-1.813	-0.363	1600	-0.879	-0.208
					2000	-0.463	-0.080						2000	-0.467	-0.078
					2000	-0.463	-0.080						2000	-0.467	-0.078
2000	1.045	15.050	-1.280	-0.260	1900	0.464	-0.003	2000	1.043	15.103	-1.274	-0.250	1900	0.468	-0.005
					2300	-1.104	-0.127						2300	-1.104	-0.120
					2300	-1.104	-0.127						2300	-1.104	-0.120
2100	1.050	21.623	4.000	-0.208	1500	2.216	-0.107	2100	1.049	21.678	3.997	-0.209	1500	2.212	-0.108
					1500	2.216	-0.107						1500	2.212	-0.108
					1800	0.568	-0.099						1800	0.570	-0.098
					1800	0.568	-0.099						1800	0.570	-0.098
					2200	-1.569	0.202						2200	-1.568	0.202
2200	1.050	27.288	3.000	-0.396	1700	1.411	-0.193	2200	1.049	27.356	2.999	-0.394	1700	1.410	-0.192
					2100	1.589	-0.203						2100	1.588	-0.202
2300	1.050	16.281	6.600	0.029	1200	2.252	0.017	2300	1.048	16.339	6.604	0.009	1200	2.252	0.015
					1300	2.133	-0.192						1300	2.136	-0.196
					2000	1.107	0.102						2000	1.108	0.095
					2000	1.107	0.102						2000	1.108	0.095
2400	1.015	10.318	-0.000	-0.000	300	2.022	0.274	2400	1.013	10.355	-0.000	0.000	300	2.020	0.270
					1500	-2.022	-0.274						1500	-2.020	-0.270

Figure 6.5: Base Case MATPOWER PF and SE Solution.

MATPOWER PF SOLUTION								SE SOLUTION							
BUS	VOLTAGE	ANGLE	Pinj	Qinj	To Bus	Plane	Qline	BUS	VOLTAGE	ANGLE	Pinj	Qinj	To Bus	Plane	Qline
100	1.050	0.000	0.760	-0.052				100	1.044	0.000	0.763	-0.078			
					200	0.102	-0.273						200	0.105	-0.285
					300	-0.002	0.211						300	0.014	0.207
					500	0.660	0.010						500	0.644	0.000
200	1.050	-0.077	0.870	-0.085				200	1.044	-0.081	0.857	-0.080			
					100	-0.102	-0.235						100	-0.105	-0.218
					400	0.446	0.189						400	0.451	0.184
					600	0.526	-0.038						600	0.511	-0.045
300	1.001	0.745	-1.800	-0.370				300	0.995	0.553	-1.805	-0.368			
					100	0.005	-0.260						100	-0.011	-0.255
					900	0.208	-0.175						900	0.189	-0.179
					2400	-2.012	0.065						2400	-1.983	0.066
400	1.012	-2.759	-0.740	-0.150				400	1.007	-2.832	-0.739	-0.148			
					200	-0.439	-0.197						200	-0.443	-0.191
					900	-0.301	0.047						900	-0.296	0.043
500	1.036	-2.911	-0.710	-0.140				500	1.031	-2.883	-0.705	-0.138			
					100	-0.651	-0.002						100	-0.636	0.007
					1000	-0.059	-0.138						1000	-0.069	-0.145
600	1.031	-5.454	-1.360	-0.280	SHUNT: -1.064			600	1.027	-5.375	-1.337	-0.273	SHUNT: -1.056		
					200	-0.514	0.030						200	-0.499	0.036
					1000	-0.846	-1.374						1000	-0.837	-1.364
700	1.045	-3.130	0.875	0.348				700	1.040	-3.135	0.881	0.350			
					800	0.875	0.348						800	0.881	0.350
800	1.012	-5.734	-1.710	-0.350				800	1.007	-5.785	-1.719	-0.355			
					700	-0.862	-0.315						700	-0.868	-0.316
					900	-0.487	0.108						900	-0.478	0.106
					1000	-0.361	-0.143						1000	-0.372	-0.145
900	1.014	-0.924	-1.750	-0.360				900	1.009	-1.015	-0.653	-0.138			
					300	-0.205	0.150						300	-0.187	0.154
					400	0.303	-0.067						400	0.298	-0.062
					800	0.498	-0.113						800	0.489	-0.111
					1100	-1.100	-0.210						1200	-1.253	-0.118
					1200	-1.246	-0.121								
1000	1.048	-2.787	-1.950	-0.400				1000	1.044	-2.718	-2.075	-0.414			
					500	0.059	0.114						500	0.070	0.121
					600	0.856	-1.243						600	0.847	-1.233
					800	0.367	0.119						800	0.379	0.123
					1100	-1.542	0.256						1105	-1.710	0.213
					1200	-1.690	0.353						1200	-1.660	0.363
1100	1.038	4.077	-0.000	-0.000				1105	1.040	4.905	-0.000	0.000			
					900	1.103	0.312						1000	1.716	0.016
					1000	1.547	-0.070						1300	-0.729	-0.059
					1300	-1.019	-0.161						1400	-0.988	0.043
					1400	-1.631	-0.082								
1200	1.032	4.790	-0.000	-0.000				1200	1.027	4.791	0.000	-0.000			
					900	1.249	0.248						900	1.257	0.248
					1000	1.696	-0.126						1000	1.666	-0.140
					1300	-0.751	-0.331						1300	-0.798	-0.317
					2300	-2.194	0.208						2300	-2.124	0.209
1300	1.050	6.592	-0.308	0.699				1300	1.045	6.734	-0.448	0.556			
					1100	1.025	0.098						1105	0.732	-0.026
					1200	0.755	0.252						1200	0.802	0.242
					2300	-2.087	0.349						2300	-1.982	0.341
1400	1.050	7.654	-1.940	0.807				1400	1.042	7.116	-2.681	0.619			
					1100	1.645	0.089						1105	0.993	-0.100
					1600	-3.585	0.718						1600	-3.674	0.719
1500	1.044	15.922	-1.500	0.460				1500	1.037	15.700	-1.525	0.467			
					1600	0.828	-0.332						1600	0.843	-0.316
					2100	-2.188	0.212						2100	-2.193	0.212
					2100	-2.188	0.212						2100	-2.193	0.212
					2400	2.049	0.367						2400	2.019	0.359
1600	1.048	15.136	0.550	0.600				1600	1.041	14.892	0.610	0.608			
					1400	3.646	-0.334						1400	3.738	-0.303
					1500	-0.826	0.304						1500	-0.841	0.290
					1700	-3.155	0.455						1700	-3.170	0.449
					1900	0.886	0.174						1900	0.882	0.172
1700	1.049	19.484	-0.000	-0.000				1700	1.042	19.317	0.000	-0.000			
					1600	3.185	-0.275						1600	3.201	-0.262
					1800	-1.799	0.135						1800	-1.810	0.123
					2200	-1.386	0.140						2200	-1.391	0.139
1800	1.050	20.847	0.670	-0.033				1800	1.043	20.704	0.686	-0.018			
					1700	1.804	-0.125						1700	1.815	-0.113
					2100	-0.567	0.046						2100	-0.565	0.047
					2100	-0.567	0.046						2100	-0.565	0.047
1900	1.041	14.093	-1.810	-0.370				1900	1.034	13.838	-1.805	-0.374			
					1600	-0.883	-0.210						1600	-0.880	-0.207
					2000	-0.463	-0.080						2000	-0.462	-0.083
					2000	-0.463	-0.080						2000	-0.462	-0.083
2000	1.045	15.050	-1.280	-0.260				2000	1.038	14.805	-1.270	-0.248			
					1900	0.464	-0.003						1900	0.463	0.002
					1900	0.464	-0.003						1900	0.463	0.002
					2300	-1.104	-0.127						2300	-1.099	-0.126
					2300	-1.104	-0.127						2300	-1.099	-0.126
2100	1.050	21.623	4.000	-0.208				2100	1.043	21.487	4.000	-0.201			
					1500	2.216	-0.107						1500	2.222	-0.102
					1500	2.216	-0.107						1500	2.222	-0.102
					1800	0.568	-0.099						1800	0.566	-0.099
					1800	0.568	-0.099						1800	0.566	-0.099
					2200	-1.569	0.202						2200	-1.575	0.200
2200	1.050	27.288	3.000	-0.396				2200	1.044	27.243	3.012	-0.381			
					1700	1.411	-0.193						1700	1.416	-0.185
					2100	1.589	-0.203						2100	1.596	-0.196
2300	1.050	16.281	6.600	0.029				2300	1.043	16.046	6.407	-0.014			
					1200	2.252	0.017						1200	2.179	-0.004
					1300	2.133	-0.192						1300	2.024	-0.212
					2000	1.107	0.102						2000	1.102	0.101
					2000	1.107	0.102						2000	1.102	0.101
2400	1.015	10.318	-0.000	-0.000				2400	1.008	10.105	-0.000	-0.000			
					300	2.022	0.274						300	1.992	0.268
					1500	-2.022	-0.274						1500	-1.993	-0.268

Figure 6.6: Branch Exclusion MATPOWER PF and SE Solution.

Iteration	Measurement ID	Current Value (pu)	Correction (pu)	New Value (pu)	Error ( $\sigma$ )
5	PF 1400,1105	1.6399	-0.6410	0.9989	49.9
5	PI 900	-1.7355	1.0831	-0.6523	39.5
5	PF 1105,1400	-1.6344	0.6401	-0.9942	33.2
5	QF 1300,1105	0.1045	-0.1524	-0.0479	17.5
5	PI 1300	-0.2986	-0.1487	-0.4473	8.7
5	QI 1400	0.8160	-0.1706	0.6454	7.5
8	PI 1400	-1.9330	-0.7986	-2.7316	32.7
8	PF 2300,1300	2.1314	-0.1551	1.9762	14.3
8	QF 1105,1000	-0.0622	0.0946	0.0325	9.9
8	PF 2300,1200	2.2526	-0.1009	2.1517	9.4
8	PF 1200,1300	-0.7532	-0.0778	-0.8310	4.5
8	PI 2300	6.6054	-0.2303	6.3751	4.5
10	PF 1105,1300	-1.0250	0.2712	-0.7539	23.4
10	QF 1400,1105	0.0678	-0.1908	-0.1230	15.1
10	QI 900	-0.3455	0.2095	-0.1360	9.6
10	PF 1600,1400	3.6539	0.0821	3.7360	10.3
10	QF 1105,1400	-0.0770	0.1393	0.0623	7.6
10	PF 1300,1200	0.7684	0.0435	0.8119	7.5
13	PF 1300,1105	1.0083	-0.2927	0.7155	25.8
13	QF 1105,1300	-0.1537	0.0975	-0.0562	7.5
13	PF 1200,2300	-2.1962	0.0837	-2.1125	6.8
13	QF 2200,1700	-0.2257	0.0411	-0.1846	4.4
15	PF 1105,1000	1.5510	0.1314	1.6824	15.9
15	PF 1300,2300	-2.0701	0.0946	-1.9755	7.3
15	PF 1200,1000	1.7023	-0.0695	1.6328	8.2
15	PF 2300,1300	1.9762	0.0411	2.0173	6.1
15	QF 1000,1105	0.2656	-0.0571	0.2084	5.2
15	PF 1200,1300	-0.8310	0.0502	-0.7808	4.9
17	PF 1000,1105	-1.5198	-0.1756	-1.6954	13.1
19	PF 1400,1600	-3.5911	-0.0809	-3.6720	4.3
21	PI 1000	-1.9462	-0.1291	-2.0753	4.2

Table 6.7: Branch Exclusion State Estimation Bad Data.



MATPOWER PF SOLUTION						SE SOLUTION										
BUS	VOLTAGE	ANGLE	Pinj	Qinj	To Bus	Pline	Qline	BUS	VOLTAGE	ANGLE	Pinj	Qinj	To Bus	Pline	Qline	
100	1.050	0.000	0.760	0.005	200	0.180	-0.288	100	1.050	0.000	0.760	0.014	200	0.181	-0.287	
					300	0.031	0.259						300	0.018	0.265	
					500	0.549	0.034						500	0.561	0.037	
200	1.050	-0.134	0.870	0.013	100	-0.180	-0.220	200	1.050	-0.135	0.755	0.001	100	-0.181	-0.220	
					400	0.604	0.258						400	0.482	0.247	
					600	0.446	-0.024						600	0.454	-0.026	
300	0.990	0.510	-1.800	-0.370	100	-0.027	-0.302	300	0.989	0.679	-2.087	-0.362	100	-0.014	-0.307	
					900	0.438	-0.141						900	0.093	-0.169	
					2400	-2.211	0.073						2400	-2.166	0.114	
400	1.000	-3.816	-0.740	-0.150	200	-0.591	-0.243	400	1.004	-2.985	-0.911	-0.148	200	-0.473	-0.248	
					900	-0.149	0.093						900	-0.438	0.100	
500	1.036	-2.391	-0.710	-0.140	100	-0.543	-0.035	500	1.035	-2.445	-0.704	-0.146	100	-0.555	-0.037	
					1000	-0.167	-0.105						1000	-0.149	-0.109	
600	1.031	-4.658	-1.360	-0.280	( SHUNT: -1.064 )			600	1.031	-4.744	-1.348	-0.272	( SHUNT: -1.063 )			
					200	-0.437	0.003						200	-0.444	0.005	
					1000	-0.923	-1.346						1000	-0.903	-1.341	
700	1.045	-3.314	0.921	0.423	800	0.921	0.423	700	1.050	-2.165	0.918	0.419	800	0.918	0.419	
800	1.007	-6.020	-1.710	-0.350	700	-0.906	-0.382	800	1.013	-4.837	-1.712	-0.349	700	-0.904	-0.379	
					900	-0.300	0.152						900	-0.448	0.160	
					1000	-0.504	-0.120						1000	-0.360	-0.130	
900	0.993	-2.756	-1.750	-0.360	300	-0.432	0.134	900	1.005	-0.232	-1.756	-0.477	300	-0.092	0.140	
					400	0.150	-0.117						400	0.443	-0.108	
					800	0.305	-0.177						800	0.457	-0.168	
					1200	-1.773	-0.200						1100	-1.207	-0.211	
													1200	-1.357	-0.131	
1000	1.047	-1.723	-1.950	-0.400	500	0.168	0.082	1000	1.047	-1.866	-1.935	-0.288	500	0.149	0.085	
					600	0.934	-1.262						600	0.914	-1.267	
					800	0.515	0.115						800	0.366	0.105	
					1105	-1.942	0.234						1100	-1.605	0.351	
					1200	-1.624	0.431						1200	-1.760	0.438	
1105	1.045	6.871	-0.000	-0.000	1000	1.950	0.059	1105	1.030	5.353	-0.000	0.000	900	1.210	0.336	
					1300	-0.581	-0.090						1000	1.611	-0.144	
					1400	-1.370	0.031						1300	-1.187	-0.170	
1200	1.025	5.625	-0.000	-0.000	900	1.781	0.471						1400	-1.634	-0.021	
					1000	1.630	-0.215						900	1.361	0.286	
					1300	-1.105	-0.428						1000	1.766	-0.186	
					2300	-2.307	0.172						1300	-0.910	-0.323	
1300	1.050	8.304	-0.344	0.712	1105	0.583	-0.004						2300	-2.218	0.223	
					1200	1.113	0.382						1100	1.195	0.127	
					2300	-2.039	0.335						1200	0.915	0.257	
1400	1.050	9.886	-1.940	0.607	1105	1.379	-0.056	1300	1.044	8.327	0.079	0.733	2300	-2.032	0.349	
					1600	-3.319	0.663						1400	1.040	9.016	
1500	1.042	17.455	-1.500	0.460	1600	0.658	-0.388						1100	1.647	0.032	
					2100	-2.207	0.179						1600	-3.662	0.700	
					2100	-2.207	0.179						1600	0.654	-0.375	
					2400	2.256	0.489						2100	-2.208	0.185	
1600	1.047	16.815	0.550	0.600	1400	3.371	-0.346						2100	-2.208	0.185	
					1500	-0.657	0.357						2400	2.209	0.425	
					1700	-3.118	0.432						1400	3.727	-0.286	
					1900	0.953	0.157						1500	-0.652	0.345	
1700	1.049	21.112	-0.000	-0.000	1600	3.148	-0.258						1700	-3.115	0.432	
					1800	-1.766	0.120						1900	0.851	0.147	
					2200	-1.381	0.137						1600	3.145	-0.253	
1800	1.050	22.449	0.670	-0.025	1700	1.772	-0.113						1800	-1.762	0.114	
					2100	-0.551	0.044						2200	-1.384	0.139	
					2100	-0.551	0.044						1700	1.767	-0.106	
1900	1.041	15.686	-1.810	-0.370	1600	-0.951	-0.190						2100	-0.556	0.048	
					2000	-0.430	-0.090						2100	-0.556	0.048	
					2000	-0.430	-0.090						1600	-0.849	-0.183	
2000	1.045	16.571	-1.280	-0.260	1900	0.431	0.006						2000	-0.431	-0.097	
					1900	0.431	0.006						2000	-0.431	-0.097	
					2300	-1.071	-0.136						1900	0.432	0.014	
					2300	-1.071	-0.136						1900	0.432	0.014	
2100	1.050	23.203	4.000	-0.130	1500	2.235	-0.070						2300	-1.076	-0.148	
					1500	2.235	-0.070						2300	-1.076	-0.148	
					1800	0.552	-0.097						1500	2.237	-0.070	
					1800	0.552	-0.097						1500	2.237	-0.070	
					2200	-1.574	0.203						1800	0.557	-0.100	
2200	1.050	28.887	3.000	-0.395	1700	1.405	-0.192						1800	0.557	-0.100	
					2100	1.595	-0.203						2200	-1.578	0.203	
2300	1.050	17.763	6.600	0.131	1200	2.370	0.106						1700	1.409	-0.186	
					1300	2.083	-0.194						2100	1.598	-0.197	
					2000	1.074	0.109							1200	2.277	0.022
					2000	1.074	0.109							1300	2.076	-0.204
2400	1.007	11.250	-0.000	-0.000	300	2.223	-0.346						2000	1.079	0.122	
					1500	-2.223	-0.346						2000	1.079	0.122	
													300	2.178	0.290	
													1500	-2.177	-0.290	

Figure 6.7: Branch Inclusion MATPOWER PF and SE Solution.

Iteration	Measurement ID	Current Value (pu)	Correction (pu)	New Value (pu)	Error ( $\sigma$ )	Iteration	Measurement ID	Current Value (pu)	Correction (pu)	New Value (pu)	Error ( $\sigma$ )
5	PF 1300,1100	0.5901	0.5827	1.1729	54.1	14	PF 1400,1100	1.3804	0.2200	1.6004	25.7
5	PF 300,900	0.4387	-0.2700	0.1686	24.3	14	PI 300	-1.7949	-0.2986	-2.0935	15.4
5	PF 1200,1300	-1.0911	0.1440	-0.9471	19.9	14	PF 2300,1200	2.3857	-0.1266	2.2590	17.4
5	QF 1100,1000	0.0617	-0.1791	-0.1174	19.0	14	PF 200,400	0.6061	-0.1126	0.4935	15.0
5	PF 400,900	-0.1512	-0.2230	-0.3742	17.0	14	PF 1500,2400	2.2577	-0.0600	2.1977	12.7
5	QF 1300,1100	0.0049	0.1566	0.1615	18.4	14	PI 400	-0.7392	-0.1683	-0.9075	10.4
5	PF 900,800	0.3198	0.1791	0.4990	17.3	14	PF 2400,1500	-2.2327	0.0667	-2.1660	9.3
5	QF 1200,900	0.4683	-0.1764	0.2920	15.3	14	QF 1200,1300	-0.4025	0.0972	-0.3054	7.2
5	PI 1400	-1.9428	0.2744	-1.6684	14.7	14	PF 1900,1600	-0.9452	0.0895	-0.8557	7.7
5	QF 1300,1200	0.3812	-0.1071	0.2741	13.4	14	QF 2400,300	0.3500	-0.0624	0.2876	7.0
5	PI 1300	-0.3609	0.4912	0.1303	7.0	14	PI 800	-1.8508	0.1385	-1.7123	4.6
8	PF 1100,1300	-0.5717	-0.7488	-1.3206	54.5	14	QI 1400	0.5968	0.1157	0.7125	5.1
8	PF 900,300	-0.4271	0.2706	-0.1565	25.9	17	PF 1100,1400	-1.3726	-0.2742	-1.6468	17.3
8	PF 900,400	0.1499	0.2813	0.4312	24.6	17	QF 1400,1600	0.6404	0.0734	0.7138	6.2
8	PF 1600,1400	3.3802	0.3396	3.7198	14.8	17	PF 900,800	0.4990	-0.0512	0.4477	5.5
8	QF 1400,1100	-0.0651	0.0888	0.0237	11.5	17	QF 1100,1300	-0.1065	-0.0546	-0.1611	4.4
8	PF 400,200	-0.5865	0.1253	-0.4611	10.2	17	PI 1900	-1.8082	0.0956	-1.7126	4.0
8	QF 1500,2400	0.4985	-0.0758	0.4227	11.8	17	QF 300,2400	0.0763	0.0443	0.1206	4.6
8	PF 1000,800	0.5235	-0.0770	0.4465	9.8	19	PI 1400	-1.6684	-0.3749	-2.0432	15.2
8	PF 1400,1600	-3.3205	-0.3357	-3.6561	8.0	19	PF 1200,1000	1.6253	0.1316	1.7570	14.4
8	QF 900,1200	-0.2023	0.0921	-0.1102	9.1	19	PF 1000,800	0.4465	-0.0908	0.3557	8.1
8	QF 1000,1100	0.2484	0.1034	0.3519	7.8	19	QF 1200,2300	0.1824	0.0432	0.2256	5.5
8	PI 800	-1.7123	-0.1384	-1.8508	6.0	19	PF 2400,300	2.2248	-0.0548	2.1700	5.2
8	QF 2400,1500	-0.3576	0.0667	-0.2909	6.3	19	QI 900	-0.3525	-0.1282	-0.4807	5.1
8	PF 1600,1900	0.9559	-0.1126	0.8432	5.3	19	PF 300,2400	-2.2172	0.0581	-2.1590	4.0
8	QF 300,900	-0.1287	-0.0575	-0.1862	5.1	22	PF 800,900	-0.2961	-0.1521	-0.4481	12.2
8	QI 1000	-0.4129	0.1264	-0.2865	5.7	22	QF 1600,1400	-0.3440	0.0611	-0.2829	4.9
11	PF 1200,900	1.7775	-0.4063	1.3711	38.7	24	PF 1000,1200	-1.6266	-0.1417	-1.7683	11.1
11	PF 1100,1000	1.9471	-0.3706	1.5764	34.9	24	PF 300,900	0.1686	-0.0693	0.0993	6.2
11	PF 900,1200	-1.7734	0.4065	-1.3669	28.6	24	PF 400,900	-0.3742	-0.0659	-0.4400	4.9
11	PF 1000,1100	-1.9545	0.3835	-1.5710	25.5	26	PF 1100,1300	-1.3206	0.1306	-1.1900	10.1
11	PI 1600	0.5469	0.2819	0.8287	10.3	26	PF 900,300	-0.1565	0.0641	-0.0924	5.9
11	PF 1300,1200	1.1219	-0.1965	0.9255	9.1	28	PF 1200,2300	-2.3026	0.0875	-2.2152	6.7
11	QF 2300,1200	0.1062	-0.0869	0.0193	10.3	30	PF 1400,1100	1.6004	0.0470	1.6474	4.9
11	PF 800,1000	-0.4952	0.1005	-0.3947	5.2						
11	QF 1100,1400	0.0379	-0.0495	-0.0116	5.1						

Table 6.8: Branch Inclusion State Estimation Bad Data.

MATPOWER PF SOLUTION							SE SOLUTION								
BUS	VOLTAGE	ANGLE	Pinj	Qinj	To Bus	Pline	Qline	BUS	VOLTAGE	ANGLE	Pinj	Qinj	To Bus	Pline	Qline
100	1.050	0.000	0.760	-0.063	200	0.010	-0.256	100	1.042	0.000	0.381	-0.076	200	0.013	-0.258
					300	-0.065	0.193						300	-0.225	0.197
					500	0.815	0.000						500	0.594	-0.015
200	1.050	-0.007	0.870	-0.121	100	-0.010	-0.252	200	1.042	-0.010	0.813	-0.137	100	-0.013	-0.243
					400	0.242	0.173						400	0.343	0.168
					600	0.638	-0.042						600	0.482	-0.062
300	1.008	1.406	-1.800	-0.370	100	0.068	-0.243	300	1.010	3.272	-1.213	-0.372	100	0.231	-0.237
					900	-0.071	-0.160						900	0.433	-0.170
					2400	-1.797	0.034						2400	-1.876	0.036
400	1.020	-1.309	-0.740	-0.150	200	-0.239	-0.199	400	1.009	-2.045	-0.704	-0.163	200	-0.339	-0.187
					900	-0.501	0.049						900	-0.366	0.024
500	1.034	-3.622	-0.710	-0.140	100	-0.802	0.026	500	1.031	-2.680	-0.713	-0.150	100	-0.587	0.018
					1000	0.092	-0.166						1000	-0.126	-0.168
600	1.029	-6.555	-1.360	-0.280	SHUNT	-1.059		600	1.030	-5.046	-1.350	-0.275	SHUNT	-1.060	
					200	-0.620	0.056						200	-0.471	0.048
					1000	-0.740	-1.395						1000	-0.879	-1.383
700	1.043	-6.635	0.944	0.400	807	0.944	0.400	700	1.049	-2.813	0.959	0.403	800	0.959	0.403
807	1.005	-9.449	-1.710	-0.350	700	-0.928	-0.358	800	1.011	-5.643	-1.933	-0.359	700	-0.943	-0.360
					907	-0.187	0.093						900	-0.586	0.130
					1000	-0.594	-0.086						1000	-0.404	-0.130
900	1.028	1.627	-0.000	-0.000	300	0.072	0.130	900	1.016	0.130	-1.712	-0.358	300	-0.426	0.162
					400	0.508	-0.053						400	0.369	-0.039
					1200	-0.579	-0.077						800	0.602	-0.117
907	0.995	-7.392	-1.750	-0.360	807	0.189	-0.130	1100	1.047	-2.279	-1.957	-0.412	1100	-1.051	-0.240
					1100	-1.939	-0.230						1200	-1.206	-0.125
1000	1.045	-4.238	-1.950	-0.400	500	-0.091	0.143	1000	1.047	-2.279	-1.957	-0.412	500	0.127	0.146
					600	0.747	-1.218						600	0.889	-1.225
					807	0.609	0.097						800	0.411	0.110
					1100	-1.322	0.274						1100	-1.615	0.216
					1200	-1.894	0.304						1200	-1.769	0.341
1100	1.032	1.700	-0.000	-0.000	907	1.948	0.553	1200	1.042	4.881	0.000	-0.000	900	1.054	0.334
					1000	1.326	-0.134						1000	1.620	-0.013
					1300	-1.389	-0.231						1300	-0.971	-0.157
					1400	-1.885	-0.188						1400	-1.703	-0.164
1200	1.036	4.234	-0.000	-0.000	900	0.580	0.104	1200	1.034	5.640	-0.000	0.000	900	1.209	0.244
					1000	1.901	-0.021						1000	1.776	-0.093
					1300	-0.393	-0.298						1300	-0.688	-0.374
					2300	-2.088	0.215						2300	-2.296	0.223
1300	1.050	5.141	-0.356	0.779	1100	1.400	0.211	1300	1.053	7.262	-0.574	0.772	1100	0.976	0.089
					1200	0.395	0.199						1200	0.692	0.291
					2300	-2.151	0.369						2300	-2.241	0.392
1400	1.050	5.830	-1.940	1.013	1100	1.903	0.233	1400	1.057	8.554	-2.031	1.025	1100	1.718	0.180
					1600	-3.843	0.780						1600	-3.749	0.845
1500	1.045	14.801	-1.500	0.460	1600	1.011	-0.290	1500	1.049	17.198	-1.503	0.496	1600	0.945	-0.293
					2100	-2.168	0.235						2100	-2.177	0.237
					2100	-2.168	0.235						2100	-2.177	0.237
					2400	1.825	0.280						2400	1.907	0.315
1600	1.048	13.856	0.550	0.600	1400	3.913	-0.325	1600	1.052	16.318	0.530	0.522	1400	3.816	-0.419
					1500	-1.009	0.268						1500	-0.943	0.268
					1700	-3.195	0.472						1700	-3.183	0.473
					1900	0.840	0.185						1900	0.840	0.201
1700	1.049	18.260	-0.000	-0.000	1600	3.226	-0.285	1700	1.053	20.673	-0.000	-0.000	1600	3.214	-0.290
					1800	-1.835	0.143						1800	-1.822	0.145
					2200	-1.392	0.142						2200	-1.392	0.145
1800	1.050	19.650	0.670	-0.035	1700	1.840	-0.132	1800	1.054	22.044	0.670	-0.038	1700	1.827	-0.135
					2100	-0.585	0.049						2100	-0.579	0.049
					2100	-0.585	0.049						2100	-0.579	0.049
1900	1.041	12.870	-1.810	-0.370	1600	-0.838	-0.222	1900	1.045	15.343	-1.818	-0.368	1600	-0.838	-0.238
					2000	-0.486	-0.074						2000	-0.490	-0.065
					2000	-0.486	-0.074						2000	-0.490	-0.065
2000	1.045	13.875	-1.280	-0.260	1900	0.487	-0.008	2000	1.048	16.353	-1.292	-0.276	1900	0.491	-0.018
					1900	0.487	-0.008						1900	0.491	-0.018
					2300	-1.127	-0.122						2300	-1.137	-0.120
					2300	-1.127	-0.122						2300	-1.137	-0.120
2100	1.050	20.451	4.000	-0.268	1500	2.196	-0.134	2100	1.054	22.830	4.001	-0.269	1500	2.205	-0.136
					1500	2.196	-0.134						1500	2.205	-0.136
					1800	0.586	-0.101						1800	0.580	-0.102
					1800	0.586	-0.101						1800	0.580	-0.102
					2200	-1.564	0.201						2200	-1.568	0.207
2200	1.050	26.096	3.000	-0.396	1700	1.417	-0.193	2200	1.053	28.454	3.004	-0.409	1700	1.416	-0.199
					2100	1.583	-0.203						2100	1.588	-0.210
2300	1.050	15.132	6.600	-0.029	1200	2.140	-0.035	2300	1.053	17.615	6.934	0.051	1200	2.359	0.043
					1300	2.200	-0.189						1300	2.294	-0.183
					2000	1.130	0.097						2000	1.141	0.096
					2000	1.130	0.097						2000	1.141	0.096
2400	1.021	9.832	-0.000	-0.000	300	1.804	0.233	2400	1.023	12.043	-0.000	0.000	300	1.884	0.254
					1500	-1.804	-0.233						1500	-1.884	-0.254

Figure 6.8: Bus Merge MATPOWER PF and SE Solution.

Iteration	Measurement ID	Current Value (pu)	Correction (pu)	New Value (pu)	Error ( $\sigma$ )	Iteration	Measurement ID	Current Value (pu)	Correction (pu)	New Value (pu)	Error ( $\sigma$ )
4	PF 1100,900	1.9580	-0.9389	1.0191	101.0	19	PF 900,300	0.0813	-0.4371	-0.3559	38.1
4	PF 900,800	0.2141	0.3242	0.5383	31.5	19	PF 1100,1300	-1.3846	0.4296	-0.9551	34.3
4	QF 1100,900	0.5640	-0.2450	0.3190	22.2	19	PF 1500,2400	1.8220	0.1377	1.9597	17.9
4	PF 1200,1000	1.8965	-0.1930	1.7035	22.4	19	PI 800	-1.7172	-0.2396	-1.9568	8.7
4	QF 1200,900	0.1013	0.1339	0.2352	14.0	19	PF 300,100	0.0775	0.0825	0.1599	6.5
4	PF 1200,2300	-2.0899	-0.1197	-2.2095	10.9	19	PI 100	0.7556	-0.2349	0.5207	4.3
4	QF 1100,1000	-0.1377	0.1148	-0.0230	12.0	22	PF 1200,1300	-0.4118	-0.2868	-0.6985	24.5
4	QF 1600,1400	-0.3257	-0.0916	-0.4173	9.0	22	PI 300	-1.5543	0.3303	-1.2240	13.8
7	PF 900,1100	-1.9426	1.0092	-0.9334	81.8	22	PI 1400	-2.2202	0.1925	-2.0277	7.5
7	PF 800,900	-0.1997	-0.3724	-0.5721	29.6	22	PF 100,300	-0.0805	-0.1371	-0.2175	7.4
7	QF 1300,1100	0.2079	-0.1144	0.0935	15.0	22	PF 1300,1100	1.0251	-0.0498	0.9753	6.9
7	PF 500,1000	0.0902	-0.1254	-0.0352	11.5	22	QF 1200,1000	-0.0240	-0.0626	-0.0867	7.0
7	QF 1400,1100	0.2398	-0.1071	0.1327	10.5	22	PI 1300	-0.3483	-0.1993	-0.5476	6.2
7	PF 500,100	-0.7970	0.1016	-0.6954	8.8	25	PF 800,1000	-0.6143	0.2198	-0.3945	17.8
7	PI 1400	-1.9317	-0.2885	-2.2202	8.4	25	PF 200,600	0.6316	-0.1666	0.4649	12.9
7	QF 1300,1200	0.2043	0.0802	0.2846	9.7	25	PF 2300,1300	2.1834	0.1301	2.3135	13.2
7	PI 300	-1.7966	0.2423	-1.5543	7.6	25	PF 900,1100	-0.9334	-0.1153	-1.0487	9.1
7	QF 1000,1100	0.2844	-0.0852	0.1992	7.5	25	PF 1000,1200	-1.8755	0.0938	-1.7817	7.4
7	PF 600,200	-0.6168	0.0772	-0.5395	7.0	25	PF 1300,2300	-2.1397	-0.1201	-2.2598	6.8
7	QF 1200,1300	-0.2826	-0.0871	-0.3697	6.4	25	PF 500,1000	-0.0352	-0.1205	-0.1557	7.4
7	PF 600,1000	-0.7474	-0.0696	-0.8170	5.2	25	PF 1400,1600	-3.8450	0.0996	-3.7454	6.3
7	PI 2300	6.5896	0.1402	6.7298	4.3	25	PF 1000,800	0.3666	0.0348	0.4014	6.7
10	PF 1200,900	0.5972	0.5495	1.1467	58.3	25	PF 500,100	-0.6954	0.1118	-0.5836	5.9
10	PF 1100,1000	1.3351	0.2343	1.5694	24.9	25	PI 2300	6.7298	0.2114	6.9412	4.4
10	QF 900,1200	-0.0617	-0.0687	-0.1303	7.8	25	QF 800,900	0.0925	0.0409	0.1334	4.4
10	PI 400	-0.7538	0.1086	-0.6452	6.7	25	PF 600,200	-0.5395	0.0845	-0.4550	4.0
10	QF 1400,1600	0.7887	0.0746	0.8633	7.1	27	PF 1400,1100	1.8935	-0.1570	1.7365	17.4
10	QF 800,1000	-0.0760	-0.0606	-0.1366	6.8	27	PF 100,500	0.6554	-0.0838	0.5716	6.9
10	QF 1500,2400	0.2867	0.0682	0.3549	6.7	27	PF 2300,1200	2.3177	0.0460	2.3638	7.1
10	PF 900,800	0.5383	0.0667	0.6049	5.5	27	QF 1400,1100	0.1327	0.0547	0.1874	5.9
10	QF 2300,1200	-0.0306	0.0503	0.0197	5.9	27	PF 1600,1500	-1.0113	0.0778	-0.9334	4.6
13	PF 900,1200	-0.5800	-0.6033	-1.1834	50.6	27	PI 400	-0.6452	-0.0793	-0.7245	4.0
13	PF 1000,1100	-1.3294	-0.2856	-1.6149	20.1	27	PF 1500,2400	1.9597	-0.0480	1.9117	4.5
13	PF 1000,800	0.6013	-0.2346	0.3666	22.7	29	PF 1100,1400	-1.8944	0.2185	-1.6758	13.8
13	PF 2300,1200	2.1320	0.1858	2.3177	19.3	29	PF 200,400	0.2542	0.0935	0.3476	7.9
13	PF 1000,500	-0.1135	0.2255	0.1121	16.0	31	PF 300,900	0.3118	0.1230	0.4348	11.2
13	PF 1000,600	0.7353	0.1559	0.8912	10.6	31	PF 900,400	0.5048	-0.1497	0.3551	10.7
13	QF 2400,300	0.2223	0.0703	0.2926	5.9	31	PF 1600,1400	3.9129	-0.1098	3.8031	12.2
13	PF 1200,1000	1.7035	0.0921	1.7955	5.1	31	PF 400,900	-0.4993	0.1475	-0.3519	9.2
16	PF 1300,1100	1.4103	-0.3852	1.0251	39.2	31	PF 900,300	-0.3559	-0.0724	-0.4283	5.5
16	PF 300,900	-0.0807	0.3924	0.3118	36.1	31	PF 600,1000	-0.8170	-0.0582	-0.8752	4.9
16	PF 1300,1200	0.4000	0.3212	0.7212	35.2	33	PF 400,200	-0.2485	-0.0982	-0.3468	7.7
16	PF 100,500	0.8125	-0.1571	0.6554	13.6	33	PF 1200,2300	-2.2095	-0.0780	-2.2875	6.1
16	QF 1100,1300	-0.2254	0.0660	-0.1594	5.1	33	QF 1500,2400	0.3549	-0.0420	0.3128	4.7
16	PF 1500,1600	1.0210	-0.0679	0.9532	5.1	35	PF 300,100	0.1599	0.0727	0.2327	7.0
16	QF 200,600	-0.0173	-0.0434	-0.0607	4.9	37	PF 2400,300	1.7993	0.0682	1.8676	7.2
16	PF 1200,900	1.1467	0.0473	1.1941	4.5	39	PF 300,2400	-1.7894	-0.0778	-1.8672	6.2
						41	PF 2400,1500	-1.8009	-0.0819	-1.8828	6.4
						43	PF 1100,1000	1.5694	0.0510	1.6204	5.6

Table 6.9: Bus Merge State Estimation Bad Data.

Iteration	Measurement ID	Current Value (pu)	Correction (pu)	New Value (pu)	Error ( $\sigma$ )
4	PI 907	-1.7438	1.1410	-0.6028	60.5
4	PI 900	0.0000	-1.1569	-1.1569	50.4

Table 6.10: Bus Split State Estimation Bad Data.

MATPOWER PF SOLUTION										SE SOLUTION									
BUS	VOLTAGE	ANGLE	Pinj	Qinj	To Bus	Pline	Qline	BUS	VOLTAGE	ANGLE	Pinj	Qinj	To Bus	Pline	Qline				
100	1.050	0.000	0.760	-0.052	200	0.102	-0.273	100	1.048	0.000	0.772	-0.046	200	0.104	-0.277				
					300	-0.002	0.211						300	-0.002	0.209				
					500	0.660	0.010						500	0.667	0.021				
200	1.050	-0.077	0.870	-0.085	100	-0.102	-0.235	200	1.048	-0.078	0.875	-0.084	100	-0.104	-0.230				
					400	0.446	0.189						400	0.452	0.185				
					600	0.526	-0.038						600	0.527	-0.039				
300	1.001	0.745	-1.800	-0.370	100	0.005	-0.260	300	1.000	0.700	-1.800	-0.371	100	0.001	-0.258				
					900	0.208	-0.175						900	0.209	-0.177				
					2400	-2.012	0.065						2400	-2.010	0.064				
400	1.012	-2.759	-0.740	-0.150	200	-0.439	-0.197	400	1.011	-2.816	-0.745	-0.146	200	-0.445	-0.193				
					900	-0.301	0.047						900	-0.300	0.047				
500	1.036	-2.911	-0.710	-0.140	100	-0.651	-0.002	500	1.033	-2.945	-0.718	-0.156	100	-0.658	-0.012				
					1000	-0.059	-0.138						1000	-0.060	-0.145				
600	1.031	-5.454	-1.360	-0.280 ( SHUNT: -1.064 )	200	-0.514	0.030	600	1.030	-5.482	-1.353	-0.270 ( SHUNT: -1.061 )	200	-0.514	0.031				
					1000	-0.846	-1.374						1000	-0.839	-1.362				
700	1.045	-3.130	0.875	0.348	800	0.875	0.348	700	1.044	-3.169	0.879	0.354	807	0.879	0.354				
800	1.012	-5.734	-1.710	-0.350	700	-0.862	-0.315	807	1.010	-5.789	-1.712	-0.344	700	-0.865	-0.320				
					900	-0.487	0.108						907	-0.486	0.116				
					1000	-0.361	-0.143						1000	-0.361	-0.139				
900	1.014	-0.924	-1.750	-0.360	300	-0.205	0.150	900	1.013	-0.985	-1.157	-0.025	300	-0.207	0.153				
					400	0.303	-0.067						400	0.302	-0.066				
					800	0.498	-0.113						1200	-1.252	-0.112				
					1100	-1.100	-0.210	907	1.011	-0.954	-0.602	-0.338	807	0.496	-0.120				
					1200	-1.246	-0.121						1100	-1.099	-0.218				
1000	1.048	-2.787	-1.950	-0.400	500	0.059	0.114	1000	1.046	-2.825	-1.956	-0.403	500	0.060	0.121				
					600	0.856	-1.243						600	0.848	-1.246				
					800	0.367	0.119						807	0.367	0.115				
					1100	-1.542	0.256						1100	-1.542	0.256				
					1200	-1.690	0.353						1200	-1.689	0.351				
1100	1.038	4.077	-0.000	-0.000	900	1.103	0.312	1100	1.036	4.065	-0.005	0.005	907	1.102	0.321				
					1000	1.547	-0.070						1000	1.547	-0.069				
					1300	-1.019	-0.161						1300	-1.023	-0.163				
					1400	-1.631	-0.082						1400	-1.631	-0.084				
1200	1.032	4.790	-0.000	-0.000	900	1.249	0.248	1200	1.030	4.778	-0.001	-0.005	900	1.256	0.241				
					1000	1.696	-0.126						1000	1.696	-0.122				
					1300	-0.751	-0.331						1300	-0.757	-0.329				
					2300	-2.194	0.208						2300	-2.196	0.206				
1300	1.050	6.592	-0.308	0.699	1100	1.025	0.098	1300	1.048	6.600	-0.297	0.696	1100	1.029	0.101				
					1200	0.755	0.252						1200	0.760	0.250				
					2300	-2.087	0.349						2300	-2.087	0.345				
1400	1.050	7.654	-1.940	0.807	1100	1.645	0.089	1400	1.048	7.654	-1.939	0.797	1100	1.644	0.092				
					1600	-3.585	0.718						1600	-3.584	0.705				
1500	1.044	15.922	-1.500	0.460	1600	0.828	-0.332	1500	1.043	15.941	-1.494	0.479	1600	0.826	-0.321				
					2100	-2.188	0.212						2100	-2.190	0.215				
					2100	-2.188	0.212						2100	-2.190	0.215				
					2400	2.049	0.367						2400	2.061	0.370				
1600	1.048	15.136	0.550	0.600	1400	3.646	-0.334	1600	1.046	15.155	0.538	0.615	1400	3.645	-0.320				
					1500	-0.826	0.304						1500	-0.825	0.293				
					1700	-3.155	0.455						1700	-3.164	0.456				
					1900	0.886	0.174						1900	0.882	0.186				
1700	1.049	19.484	-0.000	-0.000	1600	3.185	-0.275	1700	1.047	19.528	0.009	-0.000	1600	3.195	-0.273				
					1800	-1.799	0.135						1800	-1.795	0.131				
					2200	-1.386	0.140						2200	-1.391	0.142				
1800	1.050	20.847	0.670	-0.033	1700	1.804	-0.125	1800	1.049	20.891	0.676	-0.034	1700	1.800	-0.122				
					2100	-0.567	0.046						2100	-0.562	0.044				
					2100	-0.567	0.046						2100	-0.562	0.044				
1900	1.041	14.093	-1.810	-0.370	1600	-0.893	-0.210	1900	1.039	14.115	-1.811	-0.386	1600	-0.880	-0.221				
					2000	-0.463	-0.080						2000	-0.465	-0.083				
					2000	-0.463	-0.080						2000	-0.465	-0.083				
2000	1.045	15.050	-1.280	-0.260	1900	0.464	-0.003	2000	1.043	15.079	-1.275	-0.266	1900	0.466	0.000				
					1900	0.464	-0.003						1900	0.466	0.000				
					2300	-1.104	-0.127						2300	-1.104	-0.133				
					2300	-1.104	-0.127						2300	-1.104	-0.133				
2100	1.050	21.623	4.000	-0.208	1500	2.216	-0.107	2100	1.049	21.662	3.984	-0.202	1500	2.219	-0.108				
					1500	2.216	-0.107						1500	2.219	-0.108				
					1800	0.568	-0.099						1800	0.563	-0.096				
					1800	0.568	-0.099						1800	0.563	-0.096				
					2200	-1.569	0.202						2200	-1.580	0.206				
2200	1.050	27.288	3.000	-0.396	1700	1.411	-0.193	2200	1.049	27.381	3.016	-0.396	1700	1.416	-0.192				
					2100	1.589	-0.203						2100	1.600	-0.204				
2300	1.050	16.281	6.600	0.029	1200	2.252	0.017	2300	1.049	16.313	6.600	0.052	1200	2.254	0.023				
					1300	2.133	-0.192						1300	2.133	-0.186				
					2000	1.107	0.102						2000	1.107	0.108				
					2000	1.107	0.102						2000	1.107	0.108				
2400	1.015	10.318	-0.000	-0.000	300	2.022	0.274	2400	1.013	10.288	-0.015	0.001	300	2.019	0.275				
					1500	-2.022	-0.274						1500	-2.033	-0.274				

Figure 6.9: Bus Split MATPOWER PF and SE Solution.



Iteration	Measurement ID	Current Value (pu)	Correction (pu)	New Value (pu)	Error ( $\sigma$ )
4	PF 1100,1300	0.5913	-1.8146	-1.2233	113.6
4	QF 1100,1300	0.0814	-0.3348	-0.2535	22.2
4	PI 1400	-1.9388	0.3324	-1.6064	24.2
4	QF 1100,1000	0.0534	-0.2260	-0.1726	24.8
7	PF 1300,1100	0.5809	0.8253	1.4062	100.9
7	QF 1400,1100	-0.0777	0.1744	0.0967	22.1
7	PI 1300	-0.3501	1.0162	0.6661	16.0
7	QF 1600,1400	-0.3513	0.1001	-0.2512	7.6
7	PF 1000,800	0.5288	-0.0854	0.4434	7.5
7	PF 1600,1900	0.9505	-0.1100	0.8405	6.3
7	QI 1300	0.7021	0.1854	0.8874	4.8
10	PF 1400,1100	1.3756	0.4936	1.8692	79.9
10	QF 1300,1100	-0.0003	0.2731	0.2728	35.9
10	PF 900,300	-0.4462	0.1086	-0.3376	11.6
10	PI 1400	-1.6064	0.0713	-1.5351	4.9
12	PF 1100,1000	1.9435	-0.3555	1.5880	50.2
12	PF 2300,1300	2.0840	-0.1246	1.9594	12.5
12	PF 1000,1200	-1.6239	-0.0684	-1.6923	7.7
12	QF 1100,1400	0.0384	-0.1150	-0.0767	7.8
12	PF 1300,1200	1.1139	0.0581	1.1720	11.4
12	QF 1400,1600	0.6579	-0.0930	0.5650	8.0
12	PF 900,1200	-1.7743	0.0854	-1.6889	5.8
12	QF 2300,1300	-0.1826	-0.0421	-0.2246	5.0
12	PF 400,200	-0.5871	0.0641	-0.5230	3.3
14	PF 1100,1400	-1.3631	-0.5859	-1.9490	29.5
14	PF 800,1000	-0.5075	0.0850	-0.4225	5.7
14	PI 2300	6.5895	-0.0990	6.4905	5.9
17	PF 1000,1100	-1.9493	0.3821	-1.5673	23.5
17	PF 1900,1600	-0.9660	0.1274	-0.8387	5.0
17	PF 1400,1600	-3.3013	-0.0839	-3.3852	4.3
19	QF 1000,1100	0.2207	0.1359	0.3567	10.8
19	PF 2300,1300	1.9594	0.0739	2.0333	7.6
19	PF 1200,900	1.7863	-0.0538	1.7325	7.9
19	PI 1300	0.6661	-0.2055	0.4605	4.2
21	PF 1300,1100	1.4062	-0.1154	1.2908	14.4
21	PF 200,400	0.5853	-0.0476	0.5377	9.8
21	PI 1400	-1.5351	0.1095	-1.4256	4.3
23	PF 1400,1100	1.8692	0.1076	1.9768	17.9
25	PF 1300,1200	1.1720	-0.0585	1.1135	8.8
27	PF 300,900	0.4389	-0.0838	0.3551	6.3
29	PF 1600,1400	3.3859	0.0530	3.4389	5.0

Table 6.11: Bad Data and Topology Error State Estimation Bad Data.





# Chapter 7

## Conclusion

A method of topology error detection and identification using WLS SE has been presented. Various examples have been demonstrated showing the validity of this method to detect and identify topology errors. It is able to detect and identify topology errors of branch statuses and substation bus configuration. The reduction of the bus-branch model around a suspected topology error allows for fast evaluation of various bus-branch model configuration in order to identify the correct bus-branch model that matches the physical system.

### 7.1 Further Research

One area of further research is in dynamically setting the threshold used to mark suspect equipment for topology errors, section 5.1. The threshold could be adjusted based on the measurement error magnitudes and the type of measurement error (e.g. voltage magnitude, reactive or active flow and injection measurements). This could increase the accuracy in detecting suspect equipment for possible topology errors.

A second area of further research is the level of bad data processing that is performed in evaluating various bus-branch model configurations. The correct bus-branch model could be identified both by the objective value and the number of measurements identified as bad. It is recognized that bad data can conform to a topology error. Given this situation a topology error processor needs to identify the correct bus-branch model.

## 7.2 Advantages of the Method

A primary advantage to this method is that standard power system WLS SE used in an EMS can be used as the first step and the bases of the second step in identifying the topology error. Therefore, this method does not require the development or extension of the power system SE to directly handle topology errors. This also removes the addition of another application to the EMS suite of applications that must be run on regular basis. Instead, the bad data processing output of the SE program can be used to detect possible topology errors. If no topology error is detected, then no additional computations are required. If a topology error is suspected, the SE output is used as the first stage of detecting and identifying topology errors.

A second advantage is that the system does not need to be modeled at a bus-section level. To do this requires implementing new features in the WLS SE that allow the explicit modeling of circuit breakers and require the reworking of observability analysis. This also removes the need to implement different types of SE programs as in the case of a LAV topology estimator.

A third advantage is that the dependency of the detection stage on measurement location and redundancy is reduced by not identifying suspect areas based on the number of bad measurements. It is possible to test buses or branches for topology errors that contain no direct measurements.

# References

- [1] Elizete Maria Lourenco, Antonio Simoes Costa, and Kevin A. Clements. Bayesian-based hypothesis testing for topology error identification in generalized state estimation. *IEEE Transactions on Power Systems*, 19:1206 – 1215, May 2004.
- [2] F.C Schweppe and J. Wildes. Power system static-state estimation, part i: Exact model. *IEEE Transactions on Power Apparatus and Systems*, 89:120–125, January 1970.
- [3] A. Monticelli. *State Estimation In Electric Power Systems A Generalized Approach*. Kluwer Academic Publishers, Massachusetts, 1999.
- [4] J. D. Glover and M. S. Sarma. *Power System Analysis and Design*. Thomson Learning Inc., California, 2002.
- [5] A. Abur and A. G. Expósito. *Power System State Estimation*. CRC Press, New York, 2004.
- [6] A. Monticelli and A. Garcia. Reliable bad data processing for real-time state estimation. *IEEE Transactions on Power Apparatus and Systems*, 102:1126–1139, May 1983.
- [7] O. Alsac, N. Vempati, B. Stott, and A. Monticelli. Generalized state estimation. *IEEE Transactions on Power Systems*, 13:1069–1075, August 1998.
- [8] A. Garcia and P. Abreu. Fast decoupled state estimation and bad data processing. *IEEE Transactions on Power Apparatus and Systems*, 98:1645–1652, September October 1979.

- [9] Mehdi Assadian, Richard J. Goddard, H. Wayne Hong, and Dan French. Field operation experiences with on line state estimator. *IEEE Transactions on Power Systems*, 9:50–58, February 1994.
- [10] L. Mili, Th. Van Cutsem, and M. Ribbens-Pavella. Hypothesis testing identification. *IEEE Transactions on Power Apparatus and Systems*, 103:3239–3252, January 1984.
- [11] K. A. clements and P.W. Davis. Multiple bad data detectability and identifiability: A geometric approach. *IEEE Transactions on Power Delivery*, 1:355–360, July 1986.
- [12] Tlya W. Slutsker. Bad data identification in power system state estimation based on measurement compensation and linear residual calculation. *IEEE Transactions on Power Systems*, 4:53–60, February 1989.
- [13] E. Kreyszig. *Advanced Engineering Mathematics*. John Wiley and Sons, Inc., New York, 1999.
- [14] L. Mili and Th. Van Cutsem. Implementation of the hypothesis testing identification in power system state estimation. *IEEE Transactions on Power Systems*, 3:887–893, August 1988.
- [15] A. Monticelli, Felix F. Wu, and Maosong Yen. Multiple bad data identification for state estimation by combinatorial optimization. *IEEE Transactions on Power Delivery*, 1:361 – 369, July 1986.
- [16] Albert M. Sasson, Stephen T. Ehrmann, Patrick Lynch, and Louis S. Van Slyck. Automatic power system network topology determination. *IEEE Transactions on Power Apparatus and Systems*, 92:610 – 618, March / April 1987.
- [17] R.L. Lugtu, D.F. Hackett, K.C. Liu, and D.D. Might. Power system state estimation: Detection of topological errors. *IEEE Transactions on Power Apparatus and Systems*, 99:2406–2412, November / December 1980.
- [18] A. Monticelli. Modeling circuit breakers in weighted least squares state estimation. *IEEE Transactions on Power Systems*, 8:1143–1149, August 1993.

- [19] F. F. Wu and W. E. Liu. Detection of topology errors by state estimation. *IEEE Transactions on Power Systems*, 4:176–183, February 1989.
- [20] A. Monticelli. The impact of modeling short circuit branches in state estimation. *IEEE Transactions on Power Systems*, 8:1143–1149, August 1993.
- [21] E.N. Asada, A.V. Garcia, and R. Romero. Identifying multiple interacting bad data in power system state estimation. *IEEE Transactions on Power Systems*, pages 571–577, 2005.
- [22] K.A. Clements and P.W. Davis. Detection and identification of topology errors in electric power systems. *IEEE Transactions on Power Systems*, 3:1748–1753, November 1988.
- [23] A.S. Costa and F. Vieira. Topology error identification through orthogonal estimation methods and hypothesis testing. *IEEE Transactions on Power Systems*, 3:6 – 11, September 2001.
- [24] A.S. Costa, E.M. Lourenco, and K.A. Clements. Power system topological observability analysis including switching branches. *IEEE Transactions on Power Systems*, 17:250–256, May 2002.
- [25] A. Abur, H. Kim, and M.K. Celik. Identifying the unknown circuit breaker statuses in power networks. *IEEE Transactions on Power Systems*, 10:2029–2037, November 1995.
- [26] IEEE RTS Task Force of APM Subcommittee. IEEE reliability test system. *IEEE Transactions on Power Apparatus and Systems*, 98:2047–2054, November / December 1979.
- [27] R. D. Zimmerman, C. E. Murillo-Sanchez, and R. J. Thomas. Matpower’s extensible optimal power flow architecture. *Power and Energy Society General Meeting*, pages 1–7, July 2009.
- [28] randn. <http://www.mathworks.com/help/techdoc/ref/randn.html>, Date accessed September 3, 2010.

- [29] mldivide. <http://www.mathworks.com/help/techdoc/ref/mldivide.html>, Date accessed September 3, 2010.
- [30] R.N. Allan, R. Billinton, and N.M.K. Abdel-Gavad. The IEEE reliability test system - extensions to and evaluation of the generating system. *IEEE Transactions on Power Apparatus and Systems*, 98:2047–2054, November / December 1979.
- [31] R. Billinton, P.K. Vohra, and Sudhir Kumar. Effect of station originated outages in a composite system adequacy evaluation of the IEEE reliability test system. *IEEE Transactions on Power Apparatus and Systems*, 104:2649–2656, October 1985.
- [32] Q. Binh Dam, A.P. Sakis Meliopoulos, G.T. Heydt, and A. Bose. A breaker-oriented, three-phase IEEE 24-substation test system. *IEEE Transactions on Power Systems*, 25:59–67, February 2010.
- [33] IEEE RTS Task Force of APM Subcommittee. IEEE reliability test system - 1996. *IEEE Transactions on Power Systems*, 14:1010–1020, August 1999.